arXiv:2005.10579v3 [stat.ME] 29 Nov 2022

Elastic Integrative Analysis of Randomized Trial and Real-World Data for Treatment Heterogeneity Estimation

Shu Yang*, Chenyin Gao*, Donglin Zeng†, and Xiaofei Wang‡§

Abstract

We propose a test-based elastic integrative analysis of the randomized trial and real-world data to estimate treatment effect heterogeneity with a vector of known effect modifiers. When the real-world data are not subject to bias, our approach combines the trial and real-world data for efficient estimation. Utilizing the trial design, we construct a test to decide whether or not to use real-world data. We characterize the asymptotic distribution of the test-based estimator under local alternatives. We provide a data-adaptive procedure to select the test threshold that promises the smallest mean square error and an elastic confidence interval with a good finite-sample coverage property.

Keywords and phrases: Counterfactual outcome; Least favorable confidence interval; Non-regularity; Precision medicine; Pre-test estimator; Semiparametric efficiency.

1 Introduction

Precision medicine (Hamburg and Collins, 2010), which aims at customizing medical treatments to individual patient characteristics, has recently received lots of attention. A critical step toward precision medicine is to characterize the heterogeneity of treatment effect (HTE; Rothwell, 2005, Rothwell et al., 2005) entailing how patient characteristics are related to treatment effect. Randomized trials (RTs) are the gold-standard method for treatment effect evaluation because randomization of treatment ensures that treatment groups are comparable and biases are minimized to the extent possible. However, due to high costs and eligibility criteria for recruiting patients, the trial sample is often small and limited in the patient diversity, which renders the trial underpowered to estimate the HTE and unable to estimate the HTE for specific patient characteristics. On the other hand, extensive real-world (RW) data are increasingly available for research purposes, such as electronic health records, claims databases, and disease registries, with much larger sample sizes and broader demographic and diversity than RT cohorts. Several national organizations (Norris et al., 2010) and regulatory agencies (Sherman et al., 2016) have recently advocated using RW data to have a faster and less costly drug discovery process. Indeed, big data provide unprecedented opportunities for

*Department of Statistics, North Carolina State University, North Carolina 27695, U.S.A. Email: syang24@ncsu.edu.

†Department of Biostatistics, University of North Carolina at Chapel Hill

‡Department of Biostatistics and Bioinformatics, Duke University

§This research is supported by the NSF grant DMS 1811245, NIA grant 1R01AG066883, and NIEHS 1R01ES031651. The authors would also like to thank the Associate editor and anonymous reviewers for their valuable comments and suggestions to improve the quality of the paper.

new scientific discovery; however, they also present challenges with possible incomparability with RT data due to selection bias, unmeasured confounding, lack of concurrency, data quality, outcome validity, etc (US Food and Drug Administration, 2019).

The motivating application is to evaluate adjuvant chemotherapy for resected non-small cell lung cancer (NSCLC) at early-stage disease. Adjuvant chemotherapy for resected NSCLC was shown to be effective in late-stage II and IIIA disease based on RTs (Le Chevalier, 2003). However, the benefit of adjuvant chemotherapy in stage IB NSCLC disease is unclear. Cancer and Leukemia Group B (CALGB) 9633 is the only RT designed specifically for stage IB NSCLC (Strauss et al., 2008); however, it comprises about 300 patients, which was undersized to detect clinically meaningful improvements for adjuvant chemotherapy (Katz and Saad, 2009). *"Who can benefit from adjuvant chemotherapy with stage IB NSCLC?"* remains an important clinical question. An exploratory analysis of CALGB 9633 showed that patients with tumor size ≥ 4.0 cm might benefit from adjuvant chemotherapy (Strauss et al., 2008). On the other hand, the National Cancer Database (NCDB) is a clinical oncology registry database that captures the information from approximately 75% of all newly diagnosed cancer patients in the US. Our goal is to integrate the CALGB 9633 trial with a cohort selected under the same trial eligibility criteria from the NCDB. We expect that an integrated analysis of the CALGB 9633 and NCDB data can considerably improve the efficiency of the HTE estimation on adjuvant chemotherapy regarding tumor size over the RT-only analysis. Although such population-based disease registries provide rich information citing the real-world usage of adjuvant chemotherapy, the concern is the potential bias associated with RW data.

Many authors have proposed methods for generalizing treatment effects from RTs to the target population, whose covariate distribution can be characterized by the RW data (Buchanan et al., 2018, Zhao et al., 2019, Colnet et al., 2020, Lee, Yang, Dong, Wang, Zeng and Cai, 2022, Lee, Yang and Wang, 2022). When both RT and RW data provide covariate, treatment, and outcome information, there are two main approaches for integrative analysis: meta-analyses of summary statistics (e.g., Verde and Ohmann, 2015) and pooled patient data (Sobel et al., 2017). The major drawback of meta-analyses of the first kind is that they use only aggregated information and do not distinguish the roles of the RT and RW data, both having unique strengths and weaknesses. Meta-analyses of the second kind include all patients, but pooling the data from two sources breaks the randomization of treatments and relies on causal inference methods to adjust for confounding bias (e.g., Prentice et al., 2005). More importantly, one cannot rule out possible unmeasured confounding in the RW data. In addition, most existing integrative methods focused on average treatment effects (ATEs) but not on HTEs, which lies at the heart of precision medicine.

To acknowledge the advantages of the RT and RW data, we propose an elastic algorithm for combining the RT and RW data for accurate and robust estimation of the HTE function with a vector of known effect modifiers. The primary identification assumptions underpinning our method are (i) the transportability of the HTE from the RT data to the target population and (ii) the strong ignorability of treatment assignment in the RT data. Transportability is a common assumption in the trial generalizability literature, which holds if the HTE function captures all the treatment effect modifiers, or the study sample is a random sample from the target population. The well-controlled trial design can also ensure the strong ignorability of treatment assignment. If the RW sample satisfies the parallel assumptions (i) and (ii), it is comparable to the RT sample in estimating the

HTE. In this case, integrating the RW sample would increase the efficiency of HTE estimation. Toward this end, we use the semiparametric efficiency theory (Bickel et al., 1993, Robins, 1994) to derive the semiparametrically efficient integrative estimator of the HTE. However, due to many practical limitations, the RW sample may violate the desirable comparability assumption (i) or (ii). In this case, integrating the RW sample would lead to bias in HTE estimation. Utilizing the design advantage of RTs, we derive a preliminary test statistic to gauge the comparability and reliability of the RW data and decide whether or not to use the RW data in an integrative analysis. Therefore, our test-based elastic integrative estimator uses the efficient combination strategy for estimation if the violation test is insignificant and retains only the RT data if the violation test is significant.

The proposed estimator belongs to pre-test estimation by construction (Giles and Giles, 1993) and is non-regular. We consider null, local, and fixed alternative hypotheses for the pre-testing, representing three scenarios when the comparability assumption required for the RW data is zero, weakly, and strongly violated, respectively. Notably, the fixed alternative formulates the bias of the RW score of the HTE parameter to be fixed, under which the pre-test statistic goes to infinity as the sample size increases. Thus, the inference under the fixed alternative can not capture the finite-sample behavior of the test and estimator well and lacks uniform validity. A common strategy to obtain uniform inference validity for non-regular estimators is considering the local alternative, which formulates the bias of the RW score to be in the $n^{-1/2}$ neighborhood of zero. The inference under the local alternative provides a better approximation of the finite-sample behavior of the proposed estimator. Such strategies have been considered in designing trials for sample size/power calculation and in the weak instrument, partial identification, and classification literature (Staiger and Stock, 1997, Cheng, 2008, Laber and Murphy, 2011). Under the local alternative, when the testing distribution is non-degenerate, exact inference for pre-test estimation is complex because the estimator depends on the randomness of the test procedure. This issue cannot be solved by splitting the sample into two parts for testing and estimation separately (Toyoda and Wallace, 1979). The reason is that sample splitting cannot bypass the issue of the additional randomness due to pre-testing, and therefore the impact of pre-testing remains. Also, our test statistic and estimator are constructed based on the whole sample data. To consider the effect of pre-testing, we decompose the test-based elastic integrative estimator into orthogonal components; one is affected by the pre-testing, and the other is not. This step reveals the asymptotic distributions of the proposed estimator to be mixture distributions involving a truncated normal component with ellipsoid truncation and a normal component. Under this framework, we provide a data-adaptive procedure to select the threshold of the test statistic that promises the smallest mean square error (MSE) of the proposed estimator. Lastly, we propose an elastic procedure to construct confidence intervals (CIs), which are adaptive to the local and fixed alternative and have good finite-sample coverage properties.

This article is organized as follows. Section 2 introduces the basic setup, HTE, identification assumptions, and semiparametric efficient estimation. Section 3 establishes a test statistic for gauging the comparability of the RW data with the RT data, a test-based elastic integrative estimator, the asymptotic properties, and an elastic inference procedure. Section 4 presents a simulation study to evaluate the performance of the proposed estimator in terms of robustness and efficiency. Section 5 applies the proposed method to combined CALGB 9633 (RT) and NCDB (RW) data to characterize the HTE of adjuvant chemotherapy in patients with stage IB non-small cell lung cancer. We

relegate technical details and all proofs to the supplementary material.

2 Basic setup

2.1 Notation, the HTE, and two data sources

Let $A \in \{0,1\}$ be the binary treatment, Z a vector of pre-treatment covariates of interest with the first component being 1, X a vector of auxiliary variables including Z, and Y the outcome of interest. We consider Y to be continuous or binary to fix ideas, although our framework can be extended to general-type outcomes, including the survival outcome. To define causal effects, we follow the potential outcomes framework (Neyman, 1923, Rubin, 1974). Under the Stable Unit of Treatment Value assumption, let $Y(a)$ be the potential outcome had the subject been given treatment a, for $a = 0, 1$. And, by the causal consistency assumption, the observed outcome is $Y = Y(A) = AY(1) + (1 - A)Y(0)$.

Based on the potential outcomes, the individual treatment effect is $Y(1) - Y(0)$, and $\tau(Z) = \mathbb{E}\{Y(1) - Y(0) \mid Z\}$ characterizes the HTE. For a binary outcome, $\tau(Z)$ is also called the causal risk difference. In clinical settings, the parametric family of HTEs is desirable and has wide applications in precision medicine to discover optimal treatment regimes tailored to individual characteristics (Chakraborty and Moodie, 2013). We assume the HTE function to be

$$\tau(Z) = \tau_{\psi_0}(Z) = \mathbb{E}\{Y(1) - Y(0) \mid Z; \psi_0\}, \tag{1}$$

where $\psi_0 \in \mathbb{R}^p$ is a vector of unknown parameters and p is fixed.

We illustrate the HTE function in the following examples.

Example 1. (Tian et al., 2014; Shi et al., 2016) For a continuous outcome, a linear HTE function is $\tau_{\psi_0}(Z) = Z^{\mathrm{T}}\psi_0$, where each component of ψ_0 quantifies how the treatment effect varies over each Z.

Example 2. (Tian et al., 2014; Richardson et al., 2017) For a binary outcome, an HTE function for the causal risk difference is $\tau_{\psi_0}(Z) = \{\exp(Z^{\mathrm{T}}\psi_0) - 1\}/\{\exp(Z^{\mathrm{T}}\psi_0) + 1\}$, ranging from -1 to 1.

To evaluate the effect of adjuvant chemotherapy, let Y be the indication of cancer recurrence within one year of surgery. Consider the HTE function in Example 2 with $Z = (1, \text{age}, \text{tumor size})^{\mathrm{T}}$ and $\psi_0 = (\psi_{0,0}, \psi_{0,1}, \psi_{0,2})^{\mathrm{T}}$. This model entails that, on average, the treatment would increase or decrease the risk of cancer recurrence by $|\tau_{\psi_0}(Z)|$ had the patient received adjuvant chemotherapy, and the magnitude of increase depends on age and tumor size. If $Z^{\mathrm{T}}\psi_0 < 0$, it indicates that the treatment is beneficial for this patient. Moreover, if $\psi_{0,1} < 0$ and $\psi_{0,2} < 0$, then older patients with larger tumor sizes would benefit more from adjuvant chemotherapy.

We consider two independent data sources: one from the RT study and the other from the RW study. Let $\delta = 1$ denote RT participation, and let $\delta = 0$ denote RW study participation. Let V summarize the entire record of observed variables (A, X, δ, Y). The RT data consist of $\{V_i : i \in \mathcal{A}\}$ with sample size m, and the RW data consist of $\{V_i : i \in \mathcal{B}\}$ with sample size n, where $\mathcal{A}$ and $\mathcal{B}$ are sample index sets for the two data sources. Our setup requires the RT and RW samples to contain Z's information but may include different sets of auxiliary information in X. The total sample size

is $N = m + n$. Generally, n is larger than m. In our asymptotic framework, we assume both m and n go to infinity, and $m/n \to \rho$, where $0 < \rho < 1$.

For simplicity of exposition, we use the following notations throughout the paper: $\mathbb{P}_N$ denotes the empirical measure over the combined RT and RW data, $M^{\otimes 2}$ denotes MM^{T} for a vector or matrix M, $\mathbb{E}_a(\cdot)$ and $\mathbb{V}_a(\cdot)$ are the asymptotic expectation and variance of a random variable, $A_n \perp\!\!\!\perp B_n$ denotes A_n is independent of B_n, $A_n \sim B_n$ denotes that A_n follows the same distribution as B_n, and $A_n \dot{\sim} B_n$ denotes that A_n and B_n have the same asymptotic distribution as $n \to \infty$. Let $e_\delta(X) = \mathbb{P}(A = 1 \mid X, \delta)$ be the propensity score.

2.2 Identification of the HTE from the RT and RW data

The fundamental problem of causal inference is that $Y(0)$ and $Y(1)$ are not jointly observable. Therefore, the HTE is not identifiable without additional assumptions.

We view the RT sample as the gold standard for HTE estimation, satisfying the following assumption.

Assumption 1 (RT validity)**.** (i) $\mathbb{E}\{Y(1) - Y(0) \mid X, \delta = 1\} = \tau(Z)$, and (ii) $Y(a) \perp\!\!\!\perp A \mid (X, \delta = 1)$ for $a \in \{0, 1\}$ and $0 < e_1(X) < 1$ for all $(X, \delta = 1)$.

Assumption 1(i) states that the HTE function is transportable from the RT sample to the target population. This assumption is a common assumption in the data integration literature. Stronger versions of Assumption 1(i) have also been considered in the literature, including the ignorability of study participation, i.e., $\{Y(0), Y(1)\} \perp\!\!\!\perp \delta \mid X$ (Stuart et al., 2011, Buchanan et al., 2018), or the mean exchangeability, i.e., $\mathbb{E}\{Y(a) \mid X, \delta\} = \mathbb{E}\{Y(a) \mid X\}$ for $a = 0, 1$ (Dahabreh et al., 2019). Assumption 1(i) holds if Z captures the heterogeneity of effect modifiers or if the study sample is a random sample from the target population. Under the structural equation model framework, Pearl and Bareinboim (2011) provided graphical conditions for transportability. The graphical representation can aid the investigator in assessing the plausibility of Assumption 1(i). Assumption 1(ii) entails that treatment assignment in the RT study follows a randomization mechanism based on the pre-treatment variables X, and all subjects have positive probabilities of receiving each treatment. Assumption 1(ii) holds by the design of complete randomization of treatment, where the treatment is independent of the potential outcomes and covariates, i.e., $\{Y(a), X\} \perp\!\!\!\perp A \mid \delta = 1$. It also holds by the design of stratified block randomization of treatment based on discrete X, where the treatment is independent of the potential outcomes within each stratum of X. The propensity score $e_1(X)$ is known by design.

We consider a parallel assumption for the RW sample, termed RW comparability.

Assumption 2 (RW comparability)**.** (i) $\mathbb{E}\{Y(1) - Y(0) \mid X, \delta = 0\} = \tau(Z)$, and (ii) $Y(a) \perp\!\!\!\perp A \mid (X, \delta = 0)$ for $a \in \{0, 1\}$ and $0 < e_0(X) < 1$ for all $(X, \delta = 0)$.

Although Assumption 2 appears similar to Assumption 1, its implications differ substantively. Assumption 2(i) states that the HTE function is transportable from the RW sample to the target population. To make this assumption more plausible, one can use the same trial eligibility criteria to select the RW sample to ensure a sufficient overlap of the RW covariate space with the RT sample. However, this assumption can be violated in various ways. For example, RT and RW studies may

be conducted in different care settings (large academic medical centers versus smaller community hospitals), contexts (geography, policy-related or socio-structural factors), or time frames. Each of these concerns can violate Assumption 2(i). In addition, due to the lack of control of treatment assignment in RW data, Assumption 2(ii) implies that the observed covariates X capture all the confounding variables related to the treatment and outcome. This assumption may also be restrictive in practice. For example, in the NCDB cohort, the physicians or patients decided, based on experiences or preferences, whether patients received adjuvant chemotherapy after tumor resection. While the database captures many site-level and patient-level information, there may be unmeasured confounding variables that associate with the treatment selection and clinical outcome, e.g., financial status and accessibility to health care facilities.

By trial design, we assume Assumption 1 for the RT data holds throughout the paper; however, we regard Assumption 2 for the RW data as an idealistic assumption, which may be violated. If Assumption 2 holds, we will use a semiparametric efficient strategy to combine both data sources for optimal estimation. However, if Assumption 2 is violated, our proposed method will automatically detect the violation and retain only the RT data for estimation. In practice, it is important to identify a "similar" RW sample to be integrated with the RT sample. Hernán and Robins (2016) provided a framework for using big real-world data to emulate a target trial when a randomized trial is unavailable. When selecting an RW sample, we can check the rubrics for the eligibility criteria that defines the target population, treatment definitions, assignment procedures, follow-up time, outcome, and effect contrast of interest, to increase the chance of successfully integrating the RW sample with the RT sample.

Unlike our focus on testing the comparability of the RW in HTE estimation, testing transportability alone may be of more importance in some contexts. Under Assumptions 1(ii) and 2(ii), i.e., the treatment ignorability holds, possible tests can be adopted to test $\mathbb{E}\{Y(1)-Y(0) \mid X, \delta=1\} = \mathbb{E}\{Y(1)-Y(0) \mid X, \delta=0\}$, e.g., the U-statistics-based test (Luedtke et al., 2019).

Under Assumptions 1 and 2, the following identification formula holds for the HTE:

$$\mathbb{E}\left\{ \frac{AY}{e_\delta(X)} - \frac{(1-A)Y}{1-e_\delta(X)} \middle| Z, \delta \right\} = \tau(Z). \tag{2}$$

The identification formula motivates regression analysis based on the modified outcome $A\{e_\delta(X)\}^{-1}Y - (1-A)\{1-e_\delta(X)\}^{-1}Y$ to estimate the HTE. This approach involves the inverse of the treatment probability, and thus the resulting estimator may be unstable if some estimated treatment probabilities are close to zero or one. It calls for a principled way to construct improved estimators of the HTE. Rudolph and van der Laan (2017) derived the semiparametric efficiency score (SES) and bound for the average treatment effect. In the next subsection, we derive the SES of the HTE under Assumptions 1 and 2 that motivates improved estimators.

2.3 Semiparametric efficiency score

The semiparametric model consists of model (1) with the parameter of interest ψ_0 and the unspecified distribution. Assumptions 1 and 2 impose restrictions on ψ_0. To see this, define

$$H_\psi = Y - \tau_\psi(Z)A. \tag{3}$$

Intuitively, H_{ψ_0} subtracts from the subject's observed outcome Y the treatment effect of the subject's observed treatment $\tau_{\psi_0}(Z)A$, which mimics the potential outcome $Y(0)$. Formally, following Robins (1994), we can show that $\mathbb{E}(H_{\psi_0} \mid A, X, \delta) = \mathbb{E}\{Y(0) \mid A, X, \delta\}$. Therefore, by Assumptions 1 and 2, ψ_0 must satisfy the restriction*:*

$$\mathbb{E}(H_{\psi_0} \mid A, X, \delta) = \mathbb{E}(H_{\psi_0} \mid X, \delta). \tag{4}$$

For simplicity of exposition, denote

$$\mathbb{E}(H_{\psi_0} \mid X, \delta) = \mu_\delta(X), \quad \mathbb{V}(H_{\psi_0} \mid X, \delta) = \sigma^2_\delta(X),$$

where $\mu_\delta(X)$ is the outcome mean function and $\sigma^2_\delta(X)$ is the outcome variance function. By viewing (X, δ) jointly as the set of confounders, we invoke the SES of the structural nested mean model in Robins (1994). We further make a simplifying assumption that

$$\mathbb{E}(H^2_{\psi_0} \mid A, X, \delta) = \mathbb{E}(H^2_{\psi_0} \mid X, \delta), \tag{5}$$

which is a natural extension of (4). This assumption allows us to derive the SES of ψ_0 as

$$S_{\psi_0}(V) = q^*(X, \delta)\{H_{\psi_0} - \mu_\delta(X)\}\{A - e_\delta(X)\}, \quad q^*(X, \delta) = \{\partial\tau_{\psi_0}(Z)/\partial\psi\}\left\{\sigma^2_\delta(X)\right\}^{-1}, \tag{6}$$

which separates the term with the outcome, i.e., $H_{\psi_0} - \mu_\delta(X)$, and the term with the treatment, i.e., $A - e_\delta(X)$. This feature relaxes model assumptions of the nuisance functions while retaining root-n consistency in the estimation of ψ_0; see Section 2.4. Even without the simplifying assumption in (5), by the mean independence property in (4), we can verify that

$$\mathbb{E}\{S_{\psi_0}(V)\} = \mathbb{E}[q^*(X, \delta)\mathbb{E}\{H_{\psi_0} - \mu_\delta(X) \mid X, \delta\} \times \mathbb{E}\{A - e_\delta(X) \mid X, \delta\}] = 0.$$

Therefore, if (5) holds, $S_{\psi_0}(V)$ is the SES of ψ_0; if (5) does not hold, $S_{\psi_0}(V)$ is unbiased and permits robust estimation. We provide examples to elucidate the SES below before delving into robust estimation in the following subsection.

Example 3. For a continuous outcome and the HTE function given in Example 1, the SES of ψ_0 is

$$S_{\psi_0}(V) = Z\left\{\sigma^2_\delta(X)\right\}^{-1}\{H_{\psi_0} - \mu_\delta(X)\}\{A - e_\delta(X)\}.$$

For a binary outcome and the HTE function given in Example 2, the SES of ψ_0 is

$$S_{\psi_0}(V) = Z\frac{2\exp(Z^{\mathrm{T}}\psi_0)}{\{\exp(Z^{\mathrm{T}}\psi_0) + 1\}^2}[\mu_\delta(X)\{1 - \mu_\delta(X)\}]^{-1}\{H_{\psi_0} - \mu_\delta(X)\}\{A - e_\delta(X)\}.$$

Remark 1 (Comparison with other doubly robust approaches)**.** The identification formula (2) motivates the inverse probability weighted (IPW)-adjusted regression. However, IPW is known to be inefficient and sensitive to model misspecification of the propensity score. Alternatively, Kennedy (2020) proposed a pseudo-outcome regression approach using augmented IPW (AIPW) pseudo-outcomes that leverages weighting and outcome mean functions and improves the performance of

IPW-adjusted regression. The doubly robust loss function for the treatment contrast or blip function in Luedtke and van der Laan (2016) also exploits weighting and outcome mean functions. Both IPW and AIPW use weighting to remove confounding biases; differently, the SES in (6) uses the mean independence of $H_{\psi_0} - \mu_\delta(X)$ and $A - e_\delta(X)$ to construct unbiased estimating equations. The simulation study in Section S4.1 shows that the SES approach outperforms the AIPW-adjusted approach when the propensity score can be close to zero or one.

2.4 From SES to robust estimation

In principle, an efficient estimator for ψ_0 can be obtained by solving $\mathbb{P}_N S_{\text{eff},\psi}(V) = 0$. However, $S_{\text{eff},\psi}$ depends on the unknown distribution through $e_0(X)$, $\mu_\delta(X)$, and $\sigma^2_\delta(X)$, and thus solving $\mathbb{P}_N S_{\text{eff},\psi}(V) = 0$ is infeasible. Nevertheless, the state-of-art causal inference literature suggests that estimators constructed based on SES are robust to approximation errors using machine learning methods, the so-called rate double robustness; see, e.g., Chernozhukov et al. (2018) and Rotnitzky et al. (2019).

In order to obtain a robust estimator with good efficiency properties, we consider approximating the unknown functions using non-parametric or machine learning methods. In summary, our algorithm for the estimation of ψ_0 proceeds as follows.

Step 1. Obtain an estimator of $e_0(X)$ using non-parametric or machine learning methods, denoted by $\widehat{e}_0(X)$, based on $\{(A_i, X_i, \delta_i = 0) : i \in \mathcal{B}\}$.

Step 2. Obtain a preliminary estimator $\widehat{\psi}_{\text{p}}$ by solving $\sum_{i\in\mathcal{A}}[q^*(X_i, \delta_i)\{A_i - e_1(X_i)\}H_{\psi,i}] = 0$, based on $\{(A_i, X_i, Y_i, \delta_i = 1) : i \in \mathcal{A}\}$.

Step 3. Obtain the estimators of $\mu_1(X)$ and $\mu_0(X)$ using non-parametric or machine learning methods, denoted by $\widehat{\mu}_1(X)$ and $\widehat{\mu}_0(X)$, based on $\{(A_i, X_i, H_{\widehat{\psi}_{\text{p}},i},\ \delta_i = 1) : i \in \mathcal{A}\}$ and $\{(A_i, X_i, H_{\widehat{\psi}_{\text{p}},i}, \delta_i = 0) : i \in \mathcal{B}\}$, respectively.

Step 4. Let $\widehat{S}_{\text{eff},\psi}(V)$ be $S_{\text{eff},\psi}(V)$ with the unknown quantities replaced by the estimated parametric models in Steps 1 and 3. Obtain the efficient integrative estimator $\widehat{\psi}_{\text{eff}}$ by solving

$$\mathbb{P}_N \widehat{S}_\psi(V) = 0. \tag{7}$$

The estimator $\widehat{\psi}_{\text{eff}}$ depends on the approximation of nuisance functions. To establish the asymptotic properties of $\widehat{\psi}_{\text{eff}}$, we provide the regularity conditions.

Assumption 3. (i) $\|\widehat{e}_0(X) - e_0(X)\| = o_{\mathbb{P}}(1)$ and $\|\widehat{\mu}_\delta(X) - \mu_\delta(X)\| = o_{\mathbb{P}}(1)$; (ii) $\|\widehat{e}_0(X) - e_0(X)\| \times \|\widehat{\mu}_\delta(X) - \mu_\delta(X)\| = o_{\mathbb{P}}(n^{-1/2})$; and (iii) additional regularity conditions in Assumption S1.

Assumption 3 is typical regularity conditions for Z-estimation or M-estimation (van der Vaart, 2000). Assumption 3(i) states that we require the posited models to be consistent for the two nuisance functions. Assumption 3(ii) states that the *combined rate* of convergence of the posited models is $o_{\mathbb{P}}(n^{-1/2})$. Assumption S1 regularizes the complexity of the functional space. Importantly, these conditions ensure $\widehat{\psi}_{\text{eff}}$ retains the parametric-rate consistency, allowing flexible data-adaptive models and not restricting to stringent parametric models.

Theorem 1. Suppose Assumptions 1–3 hold. Then, $\widehat{\psi}_{\text{eff}}$ is root-n consistent for ψ_0 and asymptotically normal.

Theorem 1 implies that asymptotically, $\widehat{\psi}_{\text{eff}}$ can be viewed as the solution to $\mathbb{P}_N S_\psi(V) = 0$ when the nuisance functions are known. Therefore, for consistent variance estimation of $\widehat{\psi}_{\text{eff}}$, we can use the standard sandwich formula (Stefanski and Boos, 2002) or the perturbation-based resampling (Hu and Kalbfleisch, 2000), treating the nuisance functions to be known.

3 Test-based elastic integrative analysis

A major concern for integrating the RT and RW data lies in the possibly poor quality of the RW data. Then, combining the RT and RW data into an integrative analysis would lead to a biased HTE estimator. This section addresses the critical challenge of preventing any biases present in the RW data from leaking into the proposed estimator.

3.1 Detection of the RW incompatibility

We consider all assumptions in Theorem 1 hold except that Assumption 2 may be violated. We derive a test that detects the violation of this crucial assumption for using the RW data. For simplicity, we denote the SES based solely on the RT or RW data as

$$S_{\text{rt},\psi}(V) = \delta S_\psi(V),\ S_{\text{rw},\psi}(V) = (1-\delta) S_\psi(V),$$

respectively. Moreover, let $\widehat{S}_{\text{rt},\psi}(V)$ and $\widehat{S}_{\text{rw},\psi}(V)$ be $S_{\text{rt},\psi}(V)$ and $S_{\text{rw},\psi}(V)$ with the nuisance functions replaced by their estimates, and let $\mathcal{I}_{\text{rt}} = \mathbb{E}\{S_{\text{rt},\psi_0}(V)^{\otimes 2} \mid \delta = 1\}$ and $\mathcal{I}_{\text{rw}} = \mathbb{E}\{S_{\text{rw},\psi_0}(V)^{\otimes 2} \mid \delta = 0\}$ be Fisher information matrices.

We now formulate the null hypothesis H_0 for the case when Assumption 2 holds and fixed and local alternatives H_a and $\text{H}_{a,n}$ for the case when Assumption 2 is violated:

H_0 (Null) $\mathbb{E}\{S_{\text{rw},\psi_0}(V)\} = 0$.

H_a (Fixed alternative) $\mathbb{E}\{S_{\text{rw},\psi_0}(V)\} = \eta_{\text{fix}}$, where η_{fix} is a p-vector of constants with at least one nonzero component.

$\text{H}_{a,n}$ (Local alternative) $\mathbb{E}\{S_{\text{rw},\psi_0}(V)\} = n^{-1/2}\eta$, where η is a p-vector of constants with at least one nonzero component.

Considering the fixed alternative is common to establish asymptotic properties of standard estimators and tests; however, the local alternative is useful to study finite-sample properties and regularity of non-standard estimators and tests. In finite samples, the violation of Assumption 2 may be weak; e.g., there exists a hidden confounder in the RW data, but the association between the hidden confounder and the outcome or the treatment is small. In such cases, the test statistic can be small or moderate. The fixed alternative formulates the bias of the RW score to be fixed, implying that the test statistic goes to infinity with the sample size. Consequently, the fixed alternative inference can not capture the finite-sample behavior well in the cases of weak violation and does not have uniform validity. That is, there exist scenarios where the finite-sample coverage probability from standard

inference is far from the nominal level for any sample size. The local alternative asymptotics is a common approach to obtaining uniform inference validity for non-regular estimators. In the local alternative $\mathrm{H}_{a,n}$, the bias of $S_{\mathrm{rw},\psi_0}(V)$ may be small as quantified by $n^{-1/2}\eta$. The values of η represent different tracks that the bias of $S_{\mathrm{rw},\psi_0}(V)$ follows to converge to zero. We will show that the test statistic is $O_{\mathbb{P}}(1)$, thus better capturing the finite-sample behavior in the weak violation cases. The local alternative encompasses the null and fixed alternative as special cases by considering different values of η. In particular, H_0 corresponds to $\mathrm{H}_{a,n}$ with $\eta = 0$. Also, H_a corresponds to $\mathrm{H}_{a,n}$ with $\eta = \pm\infty$; hence, considering H_a alone is not informative about the finite-sample behaviors of the proposed test and estimator.

We detect biases in the RW data based on the following two key insights. First, we obtain an initial estimator $\widehat{\psi}_{\mathrm{rt}}$ by solving the estimating equation based solely on the RT data, $\sum_{i\in\mathcal{A}} \widehat{S}_{\mathrm{rt},\psi}(V_i) = 0$. It is important to emphasize that the propensity score in the RT $e_1(X)$ is known by design and, therefore, $\widehat{\psi}_{\mathrm{rt}}$ is always consistent. Second, if Assumption 2 holds for the RW data, $S_{\mathrm{rw},\psi_0}(V)$ is unbiased, but $S_{\mathrm{rw},\psi_0}(V)$ is no longer unbiased if it is violated. Therefore, large values of $n^{-1/2}\sum_{i\in\mathcal{B}} \widehat{S}_{\mathrm{rw},\widehat{\psi}_{\mathrm{rt}}}(V_i)$ provide evidence of the violation of Assumption 2.

To detect the violation of Assumption 2 for using the RW data, we construct the test statistic

$$T = \left\{ n^{-1/2} \sum_{i\in\mathcal{B}} \widehat{S}_{\mathrm{rw},\widehat{\psi}_{\mathrm{rt}}}(V_i) \right\}^{\mathrm{T}} \widehat{\Sigma}_{SS}^{-1} \left\{ n^{-1/2} \sum_{i\in\mathcal{B}} \widehat{S}_{\mathrm{rw},\widehat{\psi}_{\mathrm{rt}}}(V_i) \right\}, \tag{8}$$

where $\Sigma_{SS} = \Gamma^{\mathrm{T}}\mathcal{I}_{\mathrm{rt}}\Gamma + \mathcal{I}_{\mathrm{rw}}$ is the asymptotic variance of $n^{-1/2}\sum_{i\in\mathcal{B}} \widehat{S}_{\mathrm{rw},\widehat{\psi}_{\mathrm{rt}}}(V_i)$, $\Gamma = \mathcal{I}_{\mathrm{rt}}^{-1}\mathcal{I}_{\mathrm{rw}}\rho^{-1/2}$, and $\widehat{\Sigma}_{SS}$ is a consistent estimator for Σ_{SS}. The test statistic T measures the distance between $n^{-1/2}\sum_{i\in\mathcal{B}} S_{\mathrm{rw},\widehat{\psi}_{\mathrm{rt}}}(V_i)$ and zero. If the idealistic assumption holds, we expect T to be small. By the standard asymptotic theory, we show in the supplementary material that under H_0, $T \dot{\sim} \chi^2_p$, a Chi-square distribution with degrees of freedom p, as $n \to \infty$. This result serves to detect the violation of the assumption required for the RW data.

3.2 Elastic integration

Let $c_\gamma = \chi^2_{p,\gamma}$ be the $100(1-\gamma)$th percentile of χ^2_p. For a small γ, if $T \geq c_\gamma$, there is strong evidence to reject H_0 for the RW data; i.e., there is a detectable bias for the RW data estimator. In this case, we would only use the RT data for estimation. On the other hand, if $T < c_\gamma$, there is no strong evidence that the RW data estimator is biased; therefore, we would combine both the RT and RW data for optimal estimation. Our strategy leads to the elastic integrative estimator $\widehat{\psi}_{\mathrm{elas}}$ solving

$$\sum_{i\in\mathcal{A}\cup\mathcal{B}} \left\{ \delta_i \widehat{S}_\psi(V_i) + \mathbf{1}(T < c_\gamma)(1-\delta_i)\widehat{S}_\psi(V_i) \right\} = 0. \tag{9}$$

The choice of γ involves the bias-variance tradeoff. On the one hand, under H_0, the acceptance probability of integrating the RW data is $\mathbb{P}(T < c_\gamma) = 1-\gamma$. Therefore, for a relatively large sample size, we will accept good-quality RW data with probability $1-\gamma$ and reject good-quality RW data with type I error γ. Hence, a small γ is desirable; similarly, for $\mathrm{H}_{a,n}$ with small η. On the other hand, under $\mathrm{H}_{a,n}$ with large η, the reverse is true, and hence a large γ is desirable.

To formally investigate the tradeoff, we characterize the asymptotic distributions of the elastic

integrative estimator $\widehat{\psi}_{\text{elas}}$ under the null, fixed, and local alternatives. We do not discuss the trivial cases when $\gamma = 0$ and 1, corresponding to $\widehat{\psi}_{\text{elas}} = \widehat{\psi}_{\text{rt}}$ or $\widehat{\psi}_{\text{eff}}$. With $\gamma \in (0, 1)$, $\widehat{\psi}_{\text{elas}}$ mixes two distributions, namely, $\widehat{\psi}_{\text{rt}} \mid (T \geq c_\gamma)$ and $\widehat{\psi}_{\text{eff}} \mid (T < c_\gamma)$. Each distribution can be non-standard because the estimators and test are constructed based on the same data and, therefore, may be asymptotically dependent.

To characterize those non-standard distributions, we decompose this task into three steps. First, by the standard asymptotic theory, it follows that $T \dot{\sim} \mathcal{Z}_1^{\mathrm{T}}\mathcal{Z}_1$, where $\mathcal{Z}_1$ is a standard p-variate normal random vector, $n^{1/2}(\widehat{\psi}_{\text{rt}} - \psi_0) \dot{\sim} \mathcal{N}_{\text{rt}}$, and $n^{1/2}(\widehat{\psi}_{\text{eff}} - \psi_0) \dot{\sim} \mathcal{N}_{\text{eff}}$, where $\mathcal{N}_{\text{rt}}$ and $\mathcal{N}_{\text{eff}}$ are some p-variate normal random vectors with variances $V_{\text{rt}} = (\rho\mathcal{I}_{\text{rt}})^{-1}$ and $V_{\text{eff}} = (\rho\mathcal{I}_{\text{rt}} + \mathcal{I}_{\text{rw}})^{-1}$, respectively.

Second, we find another standard p-variate normal random vector $\mathcal{Z}_2$ that is independent of $\mathcal{Z}_1$, and decompose the normal distributions $\mathcal{N}_{\text{rt}}$ and $\mathcal{N}_{\text{eff}}$ into two orthogonal components: i) one corresponds to $\mathcal{Z}_1$ and ii) the other one corresponds to $\mathcal{Z}_2$. Importantly, component i) would be affected by the test constraints induced by $\mathcal{Z}_1^{\mathrm{T}}\mathcal{Z}_1$, but component ii) would not be affected. For $\mathcal{N}_{\text{eff}}$, we show that it is fully represented by $\mathcal{Z}_2$ as $\mathcal{N}_{\text{eff}} = -V_{\text{eff}}^{1/2}\mathcal{Z}_2$. Therefore, its distribution is not affected by $\mathcal{Z}_1^{\mathrm{T}}\mathcal{Z}_1 < c_\gamma$; that is,

$$\mathcal{N}_{\text{eff}} \mid (\mathcal{Z}_1^{\mathrm{T}}\mathcal{Z}_1 < c_\gamma) \sim -V_{\text{eff}}^{1/2}\mathcal{Z}_2.$$

For $\mathcal{N}_{\text{rt}}$, we show that $\mathcal{N}_{\text{rt}} = V_{\text{rt-eff}}^{1/2}\mathcal{Z}_1 - V_{\text{eff}}^{1/2}\mathcal{Z}_2$ with $V_{\text{rt-eff}} = V_{\text{rt}} - V_{\text{eff}}$. Due to the independence between $\mathcal{Z}_1$ and $\mathcal{Z}_2$, $\mathcal{N}_{\text{rt}} \mid (\mathcal{Z}_1^{\mathrm{T}}\mathcal{Z}_1 \geq c_\gamma)$ is a mixture distribution

$$\mathcal{N}_{\text{rt}} \mid (\mathcal{Z}_1^{\mathrm{T}}\mathcal{Z}_1 \geq c_\gamma) \sim V_{\text{rt-eff}}^{1/2}\mathcal{Z}_{c_\gamma}^{\text{t}} - V_{\text{eff}}^{1/2}\mathcal{Z}_2,$$

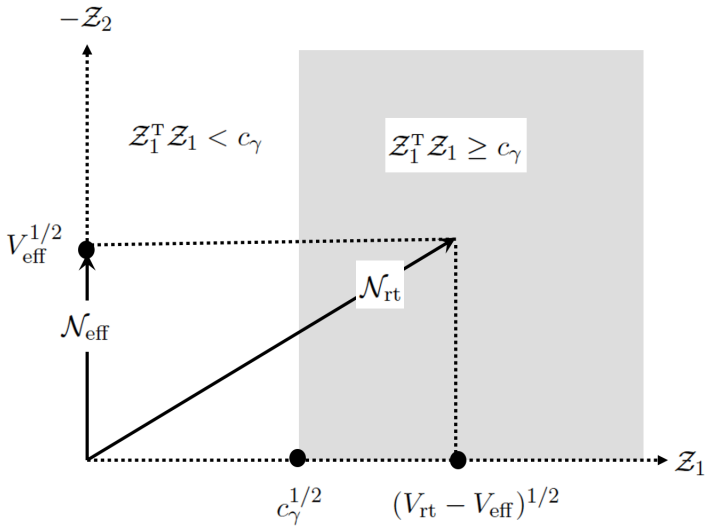
mixing a non-normal component, where $\mathcal{Z}_c^{\text{t}}$ represents the truncated normal distribution $\mathcal{Z}_1 \mid (\mathcal{Z}_1^{\mathrm{T}}\mathcal{Z}_1 \geq c)$, and a normal component. For illustration, Figure 1 demonstrates the geometry of the decomposition of distributions with scalar variables.

Third, we formally characterize the distribution of $\mathcal{Z}_c^{\text{t}}$, a multivariate normal distribution with ellipsoid truncation (Tallis, 1963, Li et al., 2018). This step enables us to quantify the asymptotic bias and variance of the proposed estimator; see Section 3.3.

Let $F_p(\cdot)$ be the cumulative distribution function (CDF) of a χ_p^2 random variable, and $F_p(\cdot;\lambda)$ be the CDF of a $\chi_p^2(\lambda)$ random variable, where χ_p^2 and $\chi_p^2(\lambda)$ are the central Chi-square distribution and the non-central Chi-square distribution with the non-centrality parameter λ, respectively. Theorem 2 summarizes the asymptotic distribution of $\widehat{\psi}_{\text{elas}}$.

Theorem 2. Suppose assumptions in Theorem 1 hold except that Assumption 2 may be violated. Let $\mathcal{Z}_1$ and $\mathcal{Z}_2$ be independent normal random vectors with mean $\mu_1 = \Sigma_{SS}^{-1/2}\eta$ and $\mu_2 = V_{\text{eff}}^{1/2}\eta$, respectively, and covariance $I_{p\times p}$. Let $\mathcal{Z}_c^{\text{t}}$ be the truncated normal distribution $\mathcal{Z}_1 \mid (\mathcal{Z}_1^{\mathrm{T}}\mathcal{Z}_1 \geq c)$. Let the elastic integrative estimator $\widehat{\psi}_{\text{elas}}$ be obtained by solving (9). Then, $n^{1/2}(\widehat{\psi}_{\text{elas}} - \psi_0)$ has a limiting mixture distribution

$$\mathcal{M}(\gamma;\eta) = \begin{cases} \mathcal{M}_1(\gamma;\eta) = V_{\text{rt-eff}}^{1/2}\mathcal{Z}_{c_\gamma}^{\text{t}} - V_{\text{eff}}^{1/2}\mathcal{Z}_2, & \text{w.p. } \xi, \\ \mathcal{M}_2(\eta) = -V_{\text{eff}}^{1/2}\mathcal{Z}_2, & \text{w.p. } 1-\xi, \end{cases} \tag{10}$$



- $\mathcal{N}_{\text{rt}} = V_{\text{rt-eff}}^{1/2}\mathcal{Z}_1 - V_{\text{eff}}^{1/2}\mathcal{Z}_2$ and $\mathcal{N}_{\text{rt}} \mid (\mathcal{Z}_1^{\mathrm{T}}\mathcal{Z}_1 \geq c_\gamma) \sim V_{\text{rt-eff}}^{1/2}\mathcal{Z}_1 \mid (\mathcal{Z}_1^{\mathrm{T}}\mathcal{Z}_1 \geq c_\gamma) - V_{\text{eff}}^{1/2}\mathcal{Z}_2$
- $\mathcal{N}_{\text{eff}} = -V_{\text{eff}}^{1/2}\mathcal{Z}_2$ and $\mathcal{N}_{\text{eff}} \mid (\mathcal{Z}_1^{\mathrm{T}}\mathcal{Z}_1 < c_\gamma) \sim \mathcal{N}_{\text{eff}}$

Figure 1: Representation of the normal distributions $\mathcal{N}_{\text{rt}}$ and $\mathcal{N}_{\text{eff}}$ based on $\mathcal{Z}_1$ and $\mathcal{Z}_2$ with $p = 1$.

a) Under H_0, $\mu_1 = \mu_2 = 0$ and $\xi = 1 - F_p(c_\gamma) = \gamma$.

b) Under H_a, $\mu_1 = \mu_2 = \pm\infty$ and $\xi = 1$; i.e., (10) reduces to a normal distribution with mean 0 and variance V_{rt}.

c) Under $\mathrm{H}_{a,n}$, $\mu_1 = \Sigma_{SS}^{-1/2}\eta$, $\mu_2 = V_{\text{eff}}^{1/2}\eta$ with $\eta \in \mathbb{R}^p$, and $\xi = 1 - F_p(c_\gamma; \lambda)$, where $\lambda = \eta^{\mathrm{T}}\Sigma_{SS}^{-1}\eta$.

In Theorem 2, $\mathcal{M}(\gamma; \eta)$ in (10) is a general characterization of the asymptotic distribution of $n^{1/2}(\widehat{\psi}_{\text{elas}} - \psi_0)$. It implies different asymptotic behaviors of $n^{1/2}(\widehat{\psi}_{\text{elas}} - \psi_0)$ depending on whether Assumption 2 is strongly, weakly, or not violated. First, H_a corresponds to the situation where Assumption 2 is strongly violated. Under H_a, T rejects the RW data (i.e., $\mathcal{Z}_1^{\mathrm{T}}\mathcal{Z}_1 \geq c_\gamma$ holds) with probability converging to one, $\mathcal{Z}_{c_\gamma}^{\text{t}}$ becomes $\mathcal{Z}_1$, and $\mathcal{M}(\gamma; \eta = \pm\infty)$ becomes $V_{\text{rt-eff}}^{1/2}\mathcal{Z}_1 - V_{\text{eff}}^{1/2}\mathcal{Z}_2$, a normal distribution with mean 0 and variance V_{rt}. As expected, under H_a, $n^{1/2}(\widehat{\psi}_{\text{elas}} - \psi_0)$ is asymptotically normal and regular. Second, H_0 and $\mathrm{H}_{a,n}$ correspond to the situations when Assumption 2 is not and weakly violated, respectively. Under H_0 and $\mathrm{H}_{a,n}$, T has positive probabilities of accepting and rejecting the RW data, $\widehat{\psi}_{\text{elas}}$ switches between $\widehat{\psi}_{\text{eff}}$ and $\widehat{\psi}_{\text{rt}}$, and $n^{1/2}(\widehat{\psi}_{\text{elas}} - \psi_0)$ follows a limiting mixing distribution $\mathcal{M}(\gamma; \eta)$, indexed by η. Although the exact form of $\mathcal{M}(\gamma; \eta)$ is complicated, the entire distribution and summary statistics such as mean, variance, and quantiles can be simulated by rejective sampling. Importantly, under H_0 and $\mathrm{H}_{a,n}$, $n^{1/2}(\widehat{\psi}_{\text{elas}} - \psi_0)$ is non-normal and non-regular. The non-regularity is determined by the local parameter η, which entails that the asymptotic distribution of $n^{1/2}(\widehat{\psi}_{\text{elas}} - \psi_0)$ may change abruptly when H_0 is slightly violated. It is worth emphasizing that the local asymptotics provides a better approach to demonstrate the finite-sample properties of the test and estimators than the fixed asymptotics does.

3.3 Asymptotic bias and MSE

Based on Theorem 2, it is essential to understand the asymptotic behaviors of $\mathcal{Z}_c^{\mathrm{t}}$ and the truncated multivariate normal distribution in general. Toward that end, we derive the moment generating functions (MGFs) of such distributions in the supplementary material, which shed light on the moments of $n^{1/2}(\widehat{\psi}_{\mathrm{elas}} - \psi_0)$.

Corollary 1 provides the analytical formula of the asymptotic bias and MSE of $n^{1/2}(\widehat{\psi}_{\mathrm{elas}} - \psi_0)$.

Corollary 1. Suppose assumptions in Theorem 1 hold except that Assumption 2 may be violated.

a) Under H_0, the bias and MSE of $n^{1/2}(\widehat{\psi}_{\mathrm{elas}} - \psi_0)$ are bias $= 0$ and mse $= V_{\mathrm{eff}} + V_{\text{rt-eff}}\{1 - F_{p+2}(c_\gamma)\}$.

b) Under H_a, the bias and MSE of $n^{1/2}(\widehat{\psi}_{\mathrm{elas}} - \psi_0)$ are bias $= 0$ and mse $= V_{\mathrm{rt}}$.

c) Under $\mathrm{H}_{a,n}$, the bias and MSE of $n^{1/2}(\widehat{\psi}_{\mathrm{elas}} - \psi_0)$ are

$$\mathrm{bias}(\gamma, \eta) = -V_{\mathrm{eff}}\eta F_{p+2}(c_\gamma; \lambda), \tag{11}$$

and

$$\begin{aligned} \mathrm{mse}(\gamma, \eta) &= V_{\mathrm{eff}} + V_{\text{rt-eff}}\{1 - F_{p+2}(c_\gamma; \lambda)\} \\ &\quad + (V_{\mathrm{eff}}\eta)^{\otimes 2}\{2F_{p+2}(c_\gamma; \lambda) - F_{p+4}(c_\gamma; \lambda)\} \end{aligned} \tag{12}$$

with $\lambda = \eta^{\mathrm{T}}\Sigma_{SS}^{-1}\eta$.

Corollary 1 enables us to demonstrate the potential advantages and disadvantages of $\widehat{\psi}_{\mathrm{elas}}$ compared with $\widehat{\psi}_{\mathrm{rt}}$ and $\widehat{\psi}_{\mathrm{eff}}$ under different scenarios. To illustrate, we consider the case of a scalar ψ_0, $V_{\mathrm{eff}} = 1$, $V_{\mathrm{rt}} = 2.5$, and $\Sigma_{SS} = 0.5$. Figure 2 shows $\mathrm{mse}(\gamma, \eta)$ as a function of η by varying $\gamma \in \{0.9, 0.5, 0.1\}$ compared to $\widehat{\psi}_{\mathrm{rt}}$. For a given $\gamma \in (0, 1)$, when η is small, $\widehat{\psi}_{\mathrm{elas}}$ is more efficient than $\widehat{\psi}_{\mathrm{rt}}$; and when η increases, the MSE of $\widehat{\psi}_{\mathrm{elas}}$ increases, exceeds, and gradually returns to the MSE of $\widehat{\psi}_{\mathrm{rt}}$. This phenomenon reveals the super-efficiency (related to the problem of non-regularity) of $\widehat{\psi}_{\mathrm{elas}}$ at small values of η at the cost of the MSE inflation for some η values. LeCam (1953) obtained an earlier result of super-efficiency for the famous Hodges estimator. Also, $\widehat{\psi}_{\mathrm{elas}}$ with a smaller γ achieves a larger deduction of the MSE at small values of η but also more considerable inflation of the MSE at big values of η compared to $\widehat{\psi}_{\mathrm{rt}}$, and vice versa. This observation motivates our adaptive selection of γ in Section 3.5 to produce an elastic integrative estimator with small bias and mean squared error for a possible value of η. Also, super-efficiency and non-regularity are the root causes for the standard asymptotic inference to fail, which motivates the proposed elastic confidence intervals to provide uniformly valid confidence intervals (Section 3.4); however, they can be conservative at certain parameter values when the sample size is small (Section 4).

Remark 2 (Sample splitting and cross fitting)**.** Sample splitting and cross fitting are helpful tactics to simplify asymptotic analyses by removing the dependence between nuisance parameter estimation and primary parameter estimation (Chernozhukov et al., 2018, Kennedy, 2020). To apply sample splitting to our context, one can divide the sample into two parts for testing and estimation

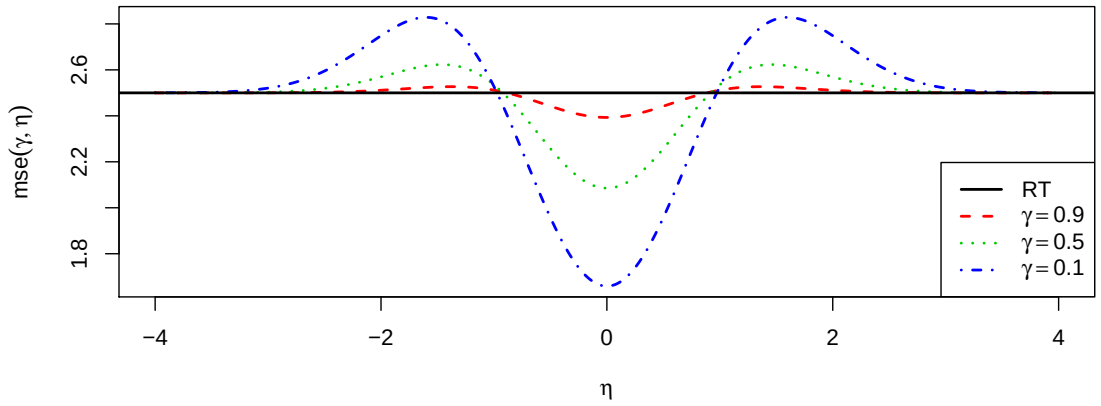


Figure 2: Illustration of the super-efficiency of $\widehat{\psi}_{\text{elas}}$ in terms of $\text{mse}(\gamma, \eta)$ as a function of η by varying $\gamma \in \{0.9(\text{dashed}), 0.5(\text{dotted}), 0.1(\text{dotdash})\}$ compared to $\widehat{\psi}_{\text{rt}}$.

separately. While sample splitting and cross fitting are beneficial in theoretical development, they may come with expenses of heavier computation and fewer data for estimating different components. Thus, we do not use sampling splitting or cross fitting as a device to establish the theoretical properties of the proposed pre-test estimator. Without sample splitting, the test and estimators are intimately related, requiring careful decompositions of the estimators into components that are asymptotically dependent and independent of the test statistic, as shown in our three steps toward Theorem 2. Also, sample splitting can not resolve the non-regularity issue of the pre-test estimator (Toyoda and Wallace, 1979). This is because sample splitting cannot bypass additional randomness due to pre-testing. Thus, the impact of pre-testing and superefficiency remains an issue; see the simulation study in Section S4.6.

Remark 3 (Soft thresholding to mitigate the non-regularity)**.** The proposed elastic integrative estimator involves an indicator function to make a binary decision to include or exclude the RW data from analysis. The indicator function serves as hard thresholding. To alleviate the non-regularity issue and refine the proposed estimator, one may use soft thresholding by imposing the smoothness of the indicator function. For example, similar to Yang and Ding (2018), one can use a smooth weight function $\Phi_\epsilon(c_\gamma - T)$ to replace $I(T < c_\gamma)$, where $\Phi_\epsilon(z)$ is the normal cumulative distribution with zero mean and variance ϵ^2. As $\epsilon \to 0$, $\Phi_\epsilon(c_\gamma - T)$ becomes closer to $I(T < c_\gamma)$. Also, as suggested by a reviewer, one can weigh the RW data based on the p-value from the test, i.e., $1 - F_p(T)$. A small p-value indicates a large bias in the RW data, and we should give the RW data less weight. Conversely, a large p-value suggests a small bias, and we should provide the RW data with more weight. The third idea is to create bootstrap replications of the elastic integrative estimator and obtain the average of the bootstrap replications to impose smoothness. Chakraborty et al. (2010) showed in simulation that soft-thresholding reduces the non-regularity of Q-learner in the dynamic treatment regime literature; however, they also provided a caveat that soft-thresholding cannot eliminate the non-regularity. Heuristically, the standard inference under the fixed alternative still provides poor finite sample coverage properties. Therefore, one still requires

the local alternative asymptotics to derive inference procedures with uniform validity as we did for the hard thresholding estimator. We will leave this topic for future research.

3.4 Inference

The nonparametric bootstrap method provides consistent inference in many cases of regular estimators. However, this feature prevents using the nonparametric bootstrap inference for $\widehat{\psi}_{\text{elas}}$ because the indicator function of the preliminary test in (9) renders $\widehat{\psi}_{\text{elas}}$ a non-smooth and non-regular estimator (Shao, 1994). We formally show in the supplementary material the inconsistency of the nonparametric bootstrap inference for $\widehat{\psi}_{\text{elas}}$. Alternatively, Laber and Murphy (2011) proposed an adaptive confidence interval for the test error in classification, a non-regular statistics, by bootstrapping the upper and lower bounds of the test error. In this article, we propose an adaptive procedure for robust inference of ψ_0 accommodating the strength of violation of Assumption 2 in finite samples.

Let e_k be a p-vector of zeros except that the kth component is one, and let $e_k^{\mathrm{T}}\psi_0$ be the kth component of ψ_0, for $k = 1, \ldots, p$. Because the asymptotic distribution of $n^{1/2}e_k^{\mathrm{T}}(\widehat{\psi}_{\text{elas}} - \psi_0)$ is different under the local and fixed alternatives, we propose different strategies for constructing CIs: under $\mathrm{H}_{a,n}$, the asymptotics is non-standard, we construct a least favorable CI that guarantees good coverage properties uniformly over possible values of the local parameter; under H_a, the asymptotics is standard, we construct the usual Wald CI based on the normal limiting distribution.

First, under $\mathrm{H}_{a,n}$, we rewrite $\mathcal{M}(\gamma;\eta)$ in (10) as $\mathcal{D}^{\mathrm{NR}}(\mu_1)+\mathcal{D}^{\mathrm{R}}$, where $\mathcal{D}^{\mathrm{NR}}(\mu_1) = V_{\text{rt-eff}}^{1/2}\mathcal{Z}_1\mathbf{1}(\mathcal{Z}_1^{\mathrm{T}}\mathcal{Z}_1 \geq c_\gamma)$ is the non-regular component with $\mathcal{Z}_1$ having mean μ_1, $\mathcal{D}^{\mathrm{R}} = -V_{\text{eff}}^{1/2}\mathcal{Z}_2$ is the regular component, and $\mathcal{D}^{\mathrm{NR}}(\mu_1)$ and $\mathcal{D}^{\mathrm{R}}$ are independent. For a fixed μ_1, let $\widehat{Q}_{k,\alpha}(\mu_1)$ be the approximated 100αth quantile of $\mathcal{D}^{\mathrm{NR}}(\mu_1)+\mathcal{D}^{\mathrm{R}}$, which can be obtained by rejective sampling. We can construct a $(1-\alpha)100\%$ confidence interval of $n^{1/2}e_k^{\mathrm{T}}(\widehat{\psi}_{\text{elas}}-\psi_0)$ as $[\widehat{Q}_{k,\alpha/2}(\mu_1), \widehat{Q}_{k,1-\alpha/2}(\mu_1)]$. Different CIs are required for different values of μ_1. To accommodate different possible values of μ_1, one solution is to construct the least favorable CI by taking the infimum of the lower bound of the CI $\widehat{Q}_{k,\alpha/2}(\mu_1)$ and the supremum of the upper bound of the CI $\widehat{Q}_{k,1-\alpha/2}(\mu_1)$ over all possible values of μ_1. However, the range of μ_1 can be vast, rendering the least favorable CI non-informative. We identify the plausible values of μ_1 following a multivariate normal distribution with mean $n^{-1/2}\widehat{\Sigma}_{SS}^{-1/2}\sum_{i\in\mathcal{B}}\widehat{S}_{\text{rw},\widehat{\psi}_{\text{rt}}}(V_i)$ and variance $I_{p\times p}$. Let $\widetilde{\alpha} = 1-(1-\alpha)^{1/2}$, such that $(1-\widetilde{\alpha})^2 = 1-\alpha$ and let $\mathcal{B}_{1-\widetilde{\alpha}}^{\mathrm{N}}$ be a $1-\widetilde{\alpha}$ bounded region of a standard p-variate normal distribution. Then,

$$\mathcal{B}_{1-\widetilde{\alpha}} = \left\{\mu_1 : \left\{n^{-1/2}\widehat{\Sigma}_{SS}^{-1/2}\sum_{i\in\mathcal{B}}\widehat{S}_{\text{rw},\widehat{\psi}_{\text{rt}}}(V_i) - \mu_1\right\} \in \mathcal{B}_{1-\widetilde{\alpha}}^{\mathrm{N}}\right\}$$

is a bounded region of μ_1 with asymptotic probability $1-\widetilde{\alpha}$. We construct the $(1-\alpha)100\%$ least favorable CI for $n^{1/2}e_k^{\mathrm{T}}(\widehat{\psi}_{\text{elas}} - \psi_0)$ as $[\inf_{\mu_1\in\mathcal{B}_{1-\widetilde{\alpha}}}\widehat{Q}_{k,\widetilde{\alpha}/2}(\mu_1), \sup_{\mu_1\in\mathcal{B}_{1-\widetilde{\alpha}}}\widehat{Q}_{k,1-\widetilde{\alpha}/2}(\mu_1)]$. Here, using the wider $(1-\widetilde{\alpha})100\%$ quantile range of $\widehat{Q}_k(\mu_1)$ instead of the $(1-\alpha)$ quantile range is necessary to guarantee the coverage of $(1-\alpha)$ due to ignoring other possible values of μ_1 outside $\mathcal{B}_{1-\tilde{\alpha}}$.

Second, under H_a, Assumption 2 is strongly violated. As shown in Theorem 2, $n^{1/2}e_k^{\mathrm{T}}(\widehat{\psi}_{\text{elas}} - \psi_0)$ is regular and asymptotically normal, denoted by $\mathcal{M}(\gamma;\pm\infty,\pm\infty)$. Therefore, a $(1-\alpha)100\%$ confidence interval of $n^{1/2}e_k^{\mathrm{T}}(\widehat{\psi}_{\text{elas}}-\psi_0)$ can be constructed based on the $100\alpha/2$- and $100(1-\alpha/2)$-th

quantiles of the normal distribution $\mathcal{M}(\gamma; \pm\infty, \pm\infty)$, denoted by $[\widehat{Q}_{k,\alpha/2}(\pm\infty), \widehat{Q}_{k,1-\alpha/2}(\pm\infty)]$.

Finally, because the least favorable CI may be unnecessarily wide under H_a, we require a strategy to distinguish between $\mathrm{H}_{a,n}$ corresponding to finite values of μ_1 and H_a corresponding to $\mu_1 = \pm\infty$. To do this, we use the test statistic T. Under $\mathrm{H}_{a,n}$, $T = O_{\mathbb{P}}(1)$; while under H_a, $T = \infty$. Therefore, we specify a sequence of thresholds $\{\kappa_n : n \geq 1\}$ that diverges to infinity as $n \to \infty$ and compare T to κ_n. Many choices of κ_n can be considered, e.g., $\kappa_n = (\log n)^{1/2}$, which is similar to the BIC criterion (Cheng, 2008, Andrews and Soares, 2010). If $T \leq \kappa_n$, we choose the local alternative strategy to construct the least favorable CI, and if $T > \kappa_n$, we choose the fixed alternative strategy to construct a normal CI, leading to an elastic CI

$$\mathrm{ECI}_{k,1-\alpha} = \begin{cases} [\inf_{\mu_1 \in \mathcal{B}_{1-\widetilde{\alpha}}} \widehat{Q}_{k,\widetilde{\alpha}/2}(\mu_1), \sup_{\mu_1 \in \mathcal{B}_{1-\widetilde{\alpha}}} \widehat{Q}_{k,1-\widetilde{\alpha}/2}(\mu_1)], & \text{if } T \leq \kappa_n, \\ [\widehat{Q}_{k,\alpha/2}(\pm\infty), \widehat{Q}_{k,1-\alpha/2}(\pm\infty)], & \text{if } T > \kappa_n. \end{cases} \tag{13}$$

Theorem 3. Suppose assumptions in Theorem 1 hold except that Assumption 2 may be violated. The asymptotic coverage rate of the elastic CI of $n^{1/2} e_k^{\mathrm{T}}(\widehat{\psi}_{\mathrm{elas}} - \psi_0)$ in (13) satisfies

$$\lim_{n\to\infty} \mathbb{P}\left\{ n^{1/2} e_k^{\mathrm{T}}(\widehat{\psi}_{\mathrm{elas}} - \psi_0) \in \mathrm{ECI}_{k,1-\alpha} \right\} \geq 1 - \alpha,$$

and the equality holds under H_a.

3.5 Adaptive selection of γ

The selection of γ involves the bas-variance tradeoff and therefore is important to determine the MSE of $\widehat{\psi}_{\mathrm{elas}}$. Corollary 1 indicates that under $\mathrm{H}_{a,n}$, the MSE of $\widehat{\psi}_{\mathrm{elas}}$ in (12) involves two terms: Term 1 is $V_{\mathrm{eff}} + V_{\text{rt-eff}}\{1 - F_{p+2}(c_\gamma; \lambda)\}$, and Term 2 involves $(V_{\mathrm{eff}}\eta)^{\otimes 2}$. If η is small, the MSE is dominated by Term 1, which can be made small if we select a small γ; while if η is large, the MSE is dominated by Term 2, which can be made small if we select a large γ.

The above observation motivates an adaptive selection of γ. We propose to estimate η by $\widehat{\eta} = n^{-1/2} \sum_{i\in\mathcal{B}} \widehat{S}_{\mathrm{rw},\widehat{\psi}_{\mathrm{rt}}}(V_i)$ and select γ that minimizes $\mathrm{mse}(\gamma; \widehat{\eta})$, where $\mathrm{mse}(\gamma; \eta)$ is given by (12) or approximated by rejective sampling. In practice, we can specify a grid of values from 0 to 1 for γ, denoted by $\mathcal{G}$, simulate the distribution of $\mathcal{M}(\gamma; \widehat{\eta})$ for all $\gamma \in \mathcal{G}$, and finally choose γ to be the one in $\mathcal{G}$ that minimizes the MSE of $\mathcal{M}(\gamma; \widehat{\eta})$. As corroborated by simulation, the selection strategy is effective in the sense that when the signal of violation is weak, the selected value of γ is small and when the signal of violation is strong, the selected value of γ is large.

4 Simulation study

We evaluate the finite sample performance of the proposed elastic estimator via simulation for robustness against unmeasured confounding and adaptive inference. Specifically, we compare the RT estimator, the efficient combining estimator, and the elastic estimator under settings that vary the strength of unmeasured confounding in the RW data. We also carry out simulation under a setting when the transportability assumption is violated in the RW data; see Section S4.3 in the supplementary material.

We first generate populations of size 10^5. For each population, we generate the covariate $X = (1, X_1, X_2, X_3)^{\mathrm{T}}$, where $X_j \sim \text{Normal}(1,1)$ for $j = 1,2,3$, and the treatment effect modifier is $Z = (1, X_1, X_2)^{\mathrm{T}}$. We generate $Y(a)$ by

$$\begin{aligned} Y(a) \mid X = \mu(X) + a \times \tau(Z) + \epsilon(a), \quad & \epsilon(a) \sim \text{Normal}(0,1), \\ \mu(X) = X_1 + X_2 + X_3, \quad & \tau(Z) = \psi_0 + \psi_1 X_1 + \psi_2 X_2, \end{aligned} \tag{14}$$

for $a = 0, 1$. Throughout the simulation, we fix ψ_0 to be zero and consider two cases for (ψ_1, ψ_2): a) zero effect modification $(\psi_1, \psi_2) = (0, 0)$ and b) nonzero effect modification $(\psi_1, \psi_2) = (1, 1)$.

We then generate two samples from the target population. We generate the RT selection indicator by $\delta \mid X \sim \text{Bernoulli}\{\pi_\delta(X)\}$, where $\text{logit}\{\pi_\delta(X)\} = -4.5 - 2X_1 - 2X_2$. Under this selection mechanism, the selection rate is around 0.6%, which results in $m \approx 620$ RT subjects. We also take a random sample of size $n \in \{2000, 5000\}$ from the population to form an RW sample. In the RT sample, the treatment assignment is $A \mid X, \delta = 1 \sim \text{Bernoulli}\{e_1(X)\}$, where $e_1(X) = 0.5$. In the RW sample, $A \mid X, \delta = 0 \sim \text{Bernoulli}\{e_0(X)\}$, where $\text{logit}\{e_0(X)\} = \alpha - X_1 - X_2 - bX_3$ with adaptively chosen α to ensure the mean of $e_0(X)$ to be around 0.5. In addition, we vary b to indicate the different strengths of unmeasured confounding in the analysis (violation of Assumption 2). The observed outcome Y in both samples is $Y = AY(1) + (1 - A)Y(0)$.

To assess the robustness of the elastic integrative estimator against unmeasured confounding, we consider the omission of X_3 in all estimators, resulting in unmeasured confounding in the RW data. The strength of unmeasured confounding is indexed by b in (14); high values of b indicate strong levels of unmeasured confounding and vice versa. We specify the range of b by 10 values in an irregular grid from 0 to 2 $\{0, 0.11, 0.23, 0.34, 0.46, 0.57, 0.69, 0.80, 1, 2\}$, which places more emphasis on the scenarios where Assumption 2 is weakly violated. We compare the following estimators for the HTE parameter ψ:

a) RT $\widehat{\psi}_{\text{rt}}$: the efficient estimator based only on the RT data solving (9) with $\mathbf{1}(T < c_\gamma) \equiv 0$;

b) Eff $\widehat{\psi}_{\text{eff}}$: the efficient integrative estimator solving (9) with $\mathbf{1}(T < c_\gamma) \equiv 1$;

c) Elastic $\widehat{\psi}_{\text{elas}}$: the proposed elastic integrative estimator solving (9) with adaptive selection of γ.

For all estimators, we estimate the propensity score function by a logistic sieve model with the power series X, X^2 and their two-way interactions (omitting X_3) and the outcome mean functions by linear sieve models with the power series X, X^2 and their two-way interactions (omitting X_3). If higher-order series is specified, it is necessary to select the series to balance the bias and variance in estimating the nuisance functions, such as using the penalized estimating equation approach (Lee, Yang, Dong, Wang, Zeng and Cai, 2022). The CIs are constructed for $\widehat{\psi}_{\text{aipw}}$, $\widehat{\psi}_{\text{rt}}$ and $\widehat{\psi}_{\text{eff}}$ based on the perturbation-based resampling with the replication size 100 and for $\widehat{\psi}_{\text{elas}}$ based on the elastic approach with $\kappa_n = (\log n)^{1/2}$. Sensitivity analysis shows that the coverage rates and widths of the CIs stay close with $\kappa_n = 0.5(\log n)^{1/2}$ (Section S4.4).

Figure 3 presents the plots of Monte Carlo biases, variances, and MSEs of estimators based on 2000 simulated datasets with numerical results reported in Table S3. Table 1 reports the coverage

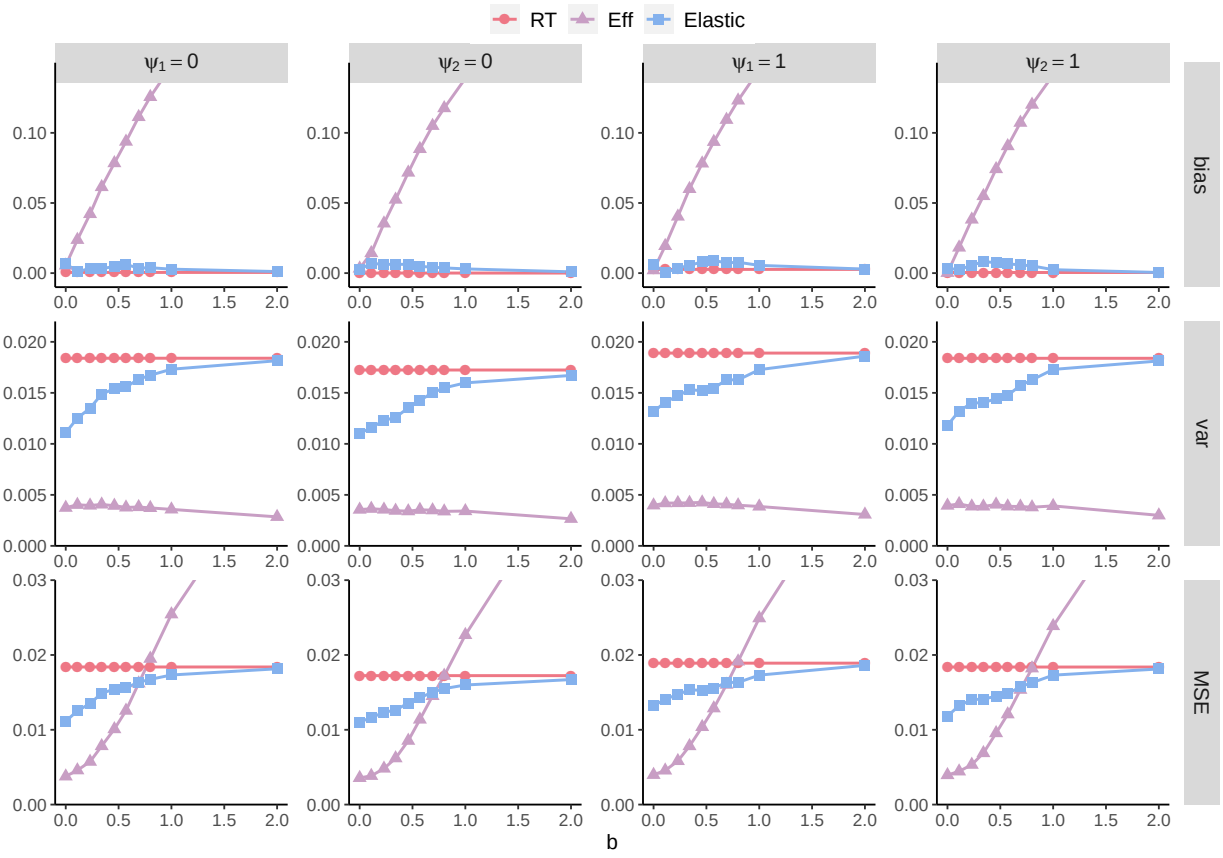


Figure 3: Summary statistics plots of estimators of (ψ_1, ψ_2) with respect to the strength of unmeasured confounding labeled by "b". In each plot, the three estimators $\widehat{\psi}_{\text{rt}}$, $\widehat{\psi}_{\text{eff}}$, and $\widehat{\psi}_{\text{elas}}$ are labeled by "RT", "Eff", and "Elastic". Each row of the plots corresponds to a different metrics: "bias" for bias, "var" for variance, "MSE" for mean square error; each column of the plots corresponds to one component of (ψ_1, ψ_2) in the two cases: $\psi_1 = 0, \psi_2 = 0$, $\psi_1 = 1$, and $\psi_2 = 1$ with $n = 2000$.

Table 1: Simulation results for coverage rates and widths of 95% confidence intervals for $\widehat{\psi}_{\text{rt}}$, $\widehat{\psi}_{\text{eff}}$, and $\widehat{\psi}_{\text{elas}}$ (labeled as "RT", "Eff", and "Elastic") in the two cases: zero effect modification $\psi_1 = \psi_2 = 0$ (left) and nonzero effect modification $\psi_1 = \psi_2 = 1$ (right) with $n = 2000$; the slightly wider ECIs for $\widehat{\psi}_{\text{eff}}$ (than CIs for $\widehat{\psi}_{\text{rt}}$) are bolded

	RT		Eff		Elastic		RT		Eff		Elastic	
	Case 1: zero effect modification						Case 2: nonzero effect modification					
b	$\psi_1 = 0$	$\psi_2 = 0$	$\psi_1 = 0$	$\psi_2 = 0$	$\psi_1 = 0$	$\psi_2 = 0$	$\psi_1 = 1$	$\psi_2 = 1$	$\psi_1 = 1$	$\psi_2 = 1$	$\psi_1 = 1$	$\psi_2 = 1$
	Coverage Rate (%)											
0	94.1	94.1	93.8	93.7	92.7	92.5	94.3	93.8	95.0	94.2	92.7	92.5
0.11	94.1	94.1	92.2	92.7	93.2	92.8	94.3	93.8	93.3	92.9	92.9	92.7
0.23	94.1	94.0	88.5	89.8	92.8	92.8	94.3	93.8	89.8	89.0	93.3	92.7
0.34	94.1	94.0	83.2	84.5	94.0	93.8	94.3	93.8	84.9	83.5	94.4	93.5
0.46	94.1	94.0	74.7	76.3	94.5	94.5	94.3	93.8	76.8	75.8	94.5	94.4
0.57	94.1	94.0	66.4	66.1	95.5	95.2	94.3	93.8	67.2	66.8	95.5	94.8
0.69	94.1	94.1	56.1	56.3	95.5	95.8	94.3	93.8	56.8	55.9	95.3	94.6
0.8	94.1	94.0	46.3	46.8	95.5	95.6	94.3	93.8	46.5	45.2	95.3	95.0
1	94.1	94.0	31.5	31.1	95.5	95.0	94.3	93.8	30.9	29.4	95.5	94.9
2	94.1	94.0	2.9	3.6	94.3	94.4	94.3	93.8	2.6	3.0	94.7	94.2
	Width ($\times 10^{-3}$)											
0	528	528	243	242	472	473	529	530	243	243	472	474
0.11	527	528	242	242	488	487	529	530	242	243	479	480
0.23	527	528	241	242	496	497	529	530	241	242	498	500
0.34	528	528	241	241	516	516	529	530	241	242	511	514
0.46	528	528	239	240	**530**	**530**	529	530	240	240	524	526
0.57	528	528	238	238	**535**	**535**	529	530	238	239	**530**	**532**
0.69	528	528	235	236	**534**	**534**	529	530	236	236	**529**	**531**
0.8	528	528	233	234	**532**	**532**	529	530	233	234	**530**	**532**
1	528	528	229	230	**529**	**529**	529	530	229	230	**530**	**532**
2	528	528	207	208	527	527	529	530	208	209	528	530

rates and widths of 95% CIs. The RT estimator $\widehat{\psi}_{\text{rt}}$ is unbiased across different scenarios, and the coverage rates are close to the nominal level. However, $\widehat{\psi}_{\text{rt}}$ has larger variances than other integrative estimators due to the small RT sample size. The efficient integrative estimator $\widehat{\psi}_{\text{eff}}$ gains efficiency over $\widehat{\psi}_{\text{rt}}$ by leveraging the large sample size of the RW data. However, the bias of $\widehat{\psi}_{\text{eff}}$ increases as b increases. Thus, $\widehat{\psi}_{\text{eff}}$ has smaller MSEs than $\widehat{\psi}_{\text{rt}}$ for small values of b but larger MSEs for large values of b. The coverage rates of the CIs for $\widehat{\psi}_{\text{eff}}$ deviate away from the nominal level as b increases. This can lead to an uncontrolled false discovery of important treatment effect modifiers (see the case of zero effect modification with $\psi_1 = \psi_2 = 0$). The elastic integrative estimator $\widehat{\psi}_{\text{elas}}$ with the adaptive selection of γ reduces $\widehat{\psi}_{\text{eff}}$'s biases across all scenarios regardless of the strength of unmeasured confounding. The challenging scenarios are indexed by b around 0.44 and 0.67, where the small biases of $\widehat{\psi}_{\text{elas}}$ occur. In these scenarios, the pre-testing (built in the elastic estimator) has difficulty in detecting the RW sample's biases. However, $\widehat{\psi}_{\text{elas}}$ with an adaptive selection of γ achieves the smallest MSE among all estimators across all scenarios (Figure 3 and Table S3).

To inspect the performance of the proposed data-adaptive selection strategy, Table S8 reports

Monte Carlo averages and standard deviations of the selected values for the local parameter η, the threshold c_γ, and the proportion of combining the RT and RW samples. As expected, $\widehat{\eta}$ increases as b increases, indicating increased biases in the RW sample. The selected γ increases (as a result, the proportion of combining the RT and RW samples decreases) as b increases, which shows the proposed adaptive selection strategy is effective. To compare the adaptive selection strategy with the fixed threshold strategy, a simulation study in Section S4.5 shows that the elastic integrative estimator $\widehat{\psi}_{\text{elas}}$ with a fixed threshold can have increased biases compared to a data-adaptive selected threshold.

The coverage rates of the ECIs for $\widehat{\psi}_{\text{elas}}$ are close to the nominal level for all settings with different values of b. The ECIs are narrower than the CIs for $\widehat{\psi}_{\text{rt}}$ when b is small ($b \leq 0.46$ for $\psi_1 = \psi_2 = 0$ and $b \leq 0.34$ for $\psi_1 = \psi_2 = 1$), are wider than the CIs for $\widehat{\psi}_{\text{rt}}$ when b increases, and become close to the CIs for $\widehat{\psi}_{\text{rt}}$ when b reaches 1 or larger. However, the conservativity of the ECIs reduces as n increases, and the ECIs can perform at least as well as the CIs for $\widehat{\psi}_{\text{rt}}$ for any b (see Table S6 for $n = 5000$).

5 An application

We illustrate the potential benefit of the proposed elastic estimator to evaluate the effect of adjuvant chemotherapy for early-stage resected non-small cell lung cancer (NSCLC) using the CALGB 9633 data and a large clinical oncology database, the NCDB. In CALGB 9633, we include 319 patients, with 163 randomly assigned to observation ($A = 0$) and 156 randomly assigned to chemotherapy ($A = 1$). The NCDB cohort is selected based on the same patient eligibility criteria as the CALGB 9633 trial; see Section S5 of the supplementary material. The comparable NCDB sample includes $15,166$ patients diagnosed with NSCLC between 2004 and 2016 in stage IB disease, with $10,903$ on observation and 4316 receiving chemotherapy after surgery. The numbers of treated and controls are relatively balanced in the CALGB 9633 trial, while they are unbalanced in the NCDB sample. We include five covariates in the analysis: gender (1 = male, 0 = female), age, the indicator for histology (1 = squamous, 0 = non-squamous), race (1 = white, 0 = non-white), and tumor size in cm. The outcome is the overall survival within three years after the surgery, i.e., $Y = 1$ if died due to all causes and $Y = 0$ otherwise. We are interested in estimating the HTE of adjuvant chemotherapy over observation after resection for the patient population with the same set of eligibility criteria as that of CALGB 9633.

Table 2 reports the covariate means by sample and treatment group. Due to treatment randomization, covariates are balanced between the treated and the control in the CALGB 9633 trial sample. While due to a lack of treatment randomization, covariates are relatively unbalanced in the NCDB sample. Older patients with histology and smaller tumors are likely to choose a conservative treatment on observation. Moreover, we can not rule out the possibility of unmeasured confounders in the NCDB sample.

We assume a linear HTE function with tumor size as the treatment effect modifier. We compare the same set of estimators and variance estimators considered in the simulation study and the efficient estimator applied to the real-world NCDB cohort, denoted by $\widehat{\psi}_{\text{rw}}$. Table 3 reports the results. Figure 4 shows the estimated treatment effect as a function of the standardized tumor

Table 2: Covariate means with standard errors in parentheses by sample and treatment group in the CALGB 9633 trial and NCDB samples

	A	N	age (years)	tumor size (cm)	male (%)	squamous (%)	white (%)
RT:	0, 1	319	60.8 (9.62)	4.60 (2.08)	63.9	39.8	89.3
CALGB 9633	1	156	60.6 (10)	4.62 (2.09)	64.1	40.4	90.4
	0	163	61.1 (9.25)	4.57 (2.07)	63.8	39.3	88.3
RW:	0, 1	15166	67.9 (10.2)	4.82 (1.71)	54.6	39.1	89.6
NCDB	1	4263	63.9 (9.23)	5.19 (1.79)	54.3	35.6	88.6
	0	10903	69.4 (10.1)	4.67 (1.65)	54.8	40.5	90.0

Table 3: Point estimate, standard error, and 95% Wald confidence interval of the causal risk difference between adjuvant chemotherapy and observation based on the CALGB 9633 trial sample and the NCDB sample: tumor size*= (tumor size−4.82)/1.72

	Intercept ($\psi_{0,1}$)				tumor size* ($\psi_{0,2}$)			
	Est.	S.E.	C.I.		Est.	S.E.	C.I.	
RT	-0.094	0.054	(-0.202,	0.015)	0.002	0.055	(-0.107,	0.111)
RW	-0.076	0.0085	(-0.093,	-0.059)	-0.029	0.009	(-0.046,	-0.011)
Eff	-0.076	0.0083	(-0.093,	-0.059)	-0.026	0.009	(-0.043,	-0.009)
Elastic	-0.076	0.0196	(-0.115,	-0.037)	-0.026	0.029	(-0.084,	0.032)

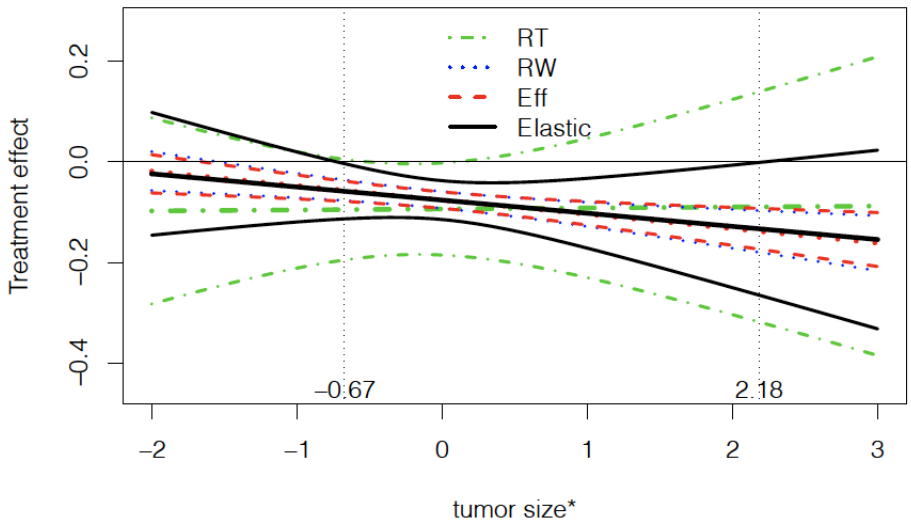


Figure 4: Estimated treatment effect as a function of the (standardized) tumor size along with the 95% Wald confidence intervals: tumor size*= (tumor size−4.82)/1.72, RT, RW, and Eff are the efficient estimator applied to the RT, RW, and combined sample, respectively, and Elastic is the proposed elastic combining estimator.

size. Due to the limited sample size of the trial sample, all components in $\widehat{\psi}_{\text{rt}}$ are not significant. Due to the large sample size of the NCDB sample, $\widehat{\psi}_{\text{rw}}$ and $\widehat{\psi}_{\text{eff}}$ are close and reveal that adjuvant chemotherapy significantly reduced cancer recurrence within three years after the surgery. Patients with larger tumor sizes benefit more from adjuvant chemotherapy. However, this finding may be subject to possible biases of the NCDB sample. In the proposed elastic integrative analysis, the test statistic is $T = 1.9$; there is no strong evidence that the NCDB presents hidden confounding in our analysis. As a result, the elastic integrative estimator $\widehat{\psi}_{\text{elas}}$ remains the same as $\widehat{\psi}_{\text{eff}}$. In reflection of the pre-testing procedure, the estimated standard error of $\widehat{\psi}_{\text{elas}}$ is larger than $\widehat{\psi}_{\text{eff}}$'s. From Figure 4, patients with tumor sizes in $[4.82 + 1.72 \times (-0.67), 4.82 + 1.72 \times (2.18)] = [3.67, 8.57]$ significantly benefit from adjuvant chemotherapy in improving overall survival within three years after the surgery.

6 Concluding remarks

The proposed elastic estimator integrates "high-quality small data" with "big data" to simultaneously leverage small but carefully controlled unbiased experiments and massive but possibly biased RW datasets for HTEs. Most causal inference methods require the no unmeasured confounding assumption. However, this assumption may not hold for the RW data due to the uncontrolled, real-world data collection mechanism and is unverifiable based only on the RW data. Utilizing the design advantage of RTs, we can gauge the reliability of the RW data and decide whether or not to use RW data in an integrative analysis.

The key assumptions underpinning our framework are the structural HTE model, i.e., Model (1), HTE transportability, and no unmeasured confounding. In practice, RTs usually consider much narrower populations than seen in the real world. Improving the generalizability or external validity of RT findings has been an important research topic in the data integration literature (e.g., Cole and Stuart, 2010, Rudolph and van der Laan, 2017, Lee, Yang, Dong, Wang, Zeng and Cai, 2022). Besides Assumption 1(i), the positivity of trial participation or the overlap of the covariate distribution between the RT and RW samples is required in the problem of generalizability. We emphasize that although, formally, we do not require the overlap assumption between the RT and RW samples, its violation renders Model (1) and transportability vulnerable. When transporting from the narrow RT sample to the broader RW sample, the reliable information of treatment effects for the non-overlapping region essentially hinges on the extrapolation from the RT sample. If there is no strong prior knowledge, Model (1) and transportability may not hold. In this case, the RT estimate and the RW estimate of the HTE can be inconsistent due to model misspecification even when there are no unmeasured confounders. See a simulation study in Section S4.3. The inconsistency of the RW estimator with the RT estimator may reflect violation of either transportability (e.g., due to model misspecification) or unmeasured confounding. Some practical strategies (e.g., matching) can be implemented to select an RW sample with sufficient overlap with the RT sample to improve their comparability and the chance of successfully integrating the information from two separate sources; see Section S5.2.

The elastic integrative estimator gains efficiency over the RT-only estimator by integrating the reliable RW data and also automatically detecting bias in the RW data and gears to the RT data.

However, the proposed estimator is non-regular and belongs to pre-test estimation by construction (Giles and Giles, 1993). To demonstrate the non-regularity issue, we characterize the distribution of the elastic integrative estimator under local alternatives, which better approximates the finite-sample behaviors. Moreover, we provide a data-adaptive selection of the threshold in the testing procedure, which guarantees small MSEs of the estimator. Nonetheless, fixing the threshold may not control bias well under $\mathrm{H}_{a,n}$; see a simulation study in Section S4.5. If the investigator prefers small biases in the elastic combining estimator, we recommend setting the lower bounds of a grid for selecting γ. Although the elastic confidence intervals demonstrate good coverage properties in our simulation under all hypotheses H_0, $\mathrm{H}_{a,n}$ and H_a, an open problem remains for the post-selection inference after a data-adaptive selection of the threshold in the testing procedure, which will be rigorously analyzed theoretically and empirically in the future study.

The proposed framework can also be extended to individualized treatment regime learning (Chu et al., 2022, Wu and Yang, 2021, 2022) and the data integration problem of combining probability and non-probability samples (Yang et al., 2019, Yang and Kim, 2019, 2020). However, an additional complication arises due to the mixed design-based and super-population inference framework, which will be overcome in future research.

Supplementary material

The R package "ElasticIntegrative" is available at https://github.com/Gaochenyin/ElasticIntegrative for implementing the proposed method. Supplementary material online includes technical details, proofs, additional simulation, the R package "ElasticIntegrative," and a README file providing instructions on downloading the R package and accessing the codes for reproducing the simulation results.

References

Andrews, D. W. and Soares, G. (2010). Inference for parameters defined by moment inequalities using generalized moment selection, *Econometrica* **78**: 119–157.

Bickel, P. J., Klaassen, C., Ritov, Y. and Wellner, J. (1993). *Efficient and Adaptive Inference in Semiparametric Models*, Johns Hopkins University Press, Baltimore.

Buchanan, A. L., Hudgens, M. G., Cole, S. R., Mollan, K. R., Sax, P. E., Daar, E. S., Adimora, A. A., Eron, J. J. and Mugavero, M. J. (2018). Generalizing evidence from randomized trials using inverse probability of sampling weights, *Journal of the Royal Statistical Society: Series A (Statistics in Society)* p. doi: 10.1111/rssa.12357.

Chakraborty, B. and Moodie, E. E. (2013). *Statistical Methods for Dynamic Treatment Regimes*, Springer, New York.

Chakraborty, B., Murphy, S. and Strecher, V. (2010). Inference for non-regular parameters in optimal dynamic treatment regimes, *Statistical Methods in Medical Research* **19**: 317–343.

Chen, X. (2007). Large sample sieve estimation of semi-nonparametric models, *Handbook of Econometrics* **6**: 5549–5632.

Cheng, X. (2008). Robust confidence intervals in nonlinear regression under weak identification, *Manuscript, Department of Economics, Yale University* .

Chernozhukov, V., Chetverikov, D., Demirer, M., Duflo, E., Hansen, C., Newey, W. and Robins, J. (2018). Double/debiased machine learning for treatment and structural parameters, *The Econometrics Journal* **21**: 1–68.

Chu, J., Lu, W. and Yang, S. (2022). Targeted optimal treatment regime learning using summary statistics, *arXiv preprint arXiv:2201.06229* .

Cole, S. R. and Stuart, E. A. (2010). Generalizing evidence from randomized clinical trials to target populations: The ACTG 320 trial, *American Journal of Epidemiology* **172**: 107–115.

Colnet, B., Mayer, I., Chen, G., Dieng, A., Li, R., Varoquaux, G., Vert, J.-P., Josse, J. and Yang, S. (2020). Causal inference methods for combining randomized trials and observational studies: a review, *arXiv preprint arXiv:2011.08047* .

Dahabreh, I. J., Robertson, S. E., Tchetgen, E. J., Stuart, E. A. and Hernán, M. A. (2019). Generalizing causal inferences from individuals in randomized trials to all trial-eligible individuals, *Biometrics* **75**: 685–694.

Giles, J. A. and Giles, D. E. (1993). Pre-test estimation and testing in econometrics: recent developments, *Journal of Economic Surveys* **7**: 145–197.

Hamburg, M. A. and Collins, F. S. (2010). The path to personalized medicine, *New England Journal of Medicine* **363**: 301–304.

Hernán, M. A. and Robins, J. M. (2016). Using big data to emulate a target trial when a randomized trial is not available, *American Journal of Epidemiology* **183**: 758–764.

Hu, F. and Kalbfleisch, J. D. (2000). The estimating function bootstrap, *Canadian Journal of Statistics* **28**: 449–481.

Katz, A. and Saad, E. D. (2009). CALGB 9633: an underpowered trial with a methodologically questionable conclusion, *Journal of Clinical Oncology* **27**: 2300–2301.

Kennedy, E. H. (2020). Optimal doubly robust estimation of heterogeneous causal effects, *arXiv preprint arXiv:2004.14497* .

Laber, E. B. and Murphy, S. A. (2011). Adaptive confidence intervals for the test error in classification, *Journal of the American Statistical Association* **106**: 904–913.

Le Chevalier, T. (2003). Results of the Randomized International Adjuvant Lung Cancer Trial (IALT): Cisplatin-based chemotherapy (CT) vs no CT in 1867 patients with resected non-small cell lung cancer (NSCLC), *Lung Cancer* **21**: 238–238.

LeCam, L. (1953). On some asymptotic properties of maximum likelihood estimates and related bayes estimates, *University of California Publications in Statistics* **1**: 277–330.

Lee, D., Yang, S., Dong, L., Wang, X., Zeng, D. and Cai, J. (2022). Improving trial generalizability using observational studies, *Biometrics* p. doi:10.1111/biom.13609.

Lee, D., Yang, S. and Wang, X. (2022). Generalizable survival analysis of randomized controlled trials with observational studies, *arXiv preprint arXiv:2201.06595* .

Li, X., Ding, P. and Rubin, D. B. (2018). Asymptotic theory of rerandomization in treatment–control experiments, *Proceedings of the National Academy of Sciences* **115**: 9157–9162.

Luedtke, A., Carone, M. and van der Laan, M. J. (2019). An omnibus non-parametric test of equality in distribution for unknown functions, *Journal of the Royal Statistical Society: Series B (Statistical Methodology)* **81**: 75–99.

Luedtke, A. R. and van der Laan, M. J. (2016). Super-learning of an optimal dynamic treatment rule, *The International Journal of Biostatistics* **12**: 305–332.

Newey, W. K. (1997). Convergence rates and asymptotic normality for series estimators, *Journal of Econometrics* **79**: 147–168.

Neyman, J. (1923). Sur les applications de la thar des probabilities aux experiences Agaricales: Essay de principle. English translation of excerpts by Dabrowska, D. and Speed, T., *Statistical Science* **5**: 465–472.

Norris, S., Atkins, D., Bruening, W., Fox, S., Johnson, E., Kane, R., Morton, S. C., Oremus, M., Ospina, M., Randhawa, G., Schoelles, K., Shekelle, P. and Viswanathan, M. (2010). Selecting observational studies for comparing medical interventions, *Methods Guide for Effectiveness and Comparative Effectiveness Reviews [Internet]*, Agency for Healthcare Research and Quality (US).

Pearl, J. and Bareinboim, E. (2011). Transportability of causal and statistical relations: A formal approach, *Data Mining Workshops (ICDMW), 2011 IEEE 11th International Conference on*, IEEE, pp. 540–547.

Prentice, R. L., Langer, R., Stefanick, M. L., Howard, B. V., Pettinger, M., Anderson, G., Barad, D., Curb, J. D., Kotchen, J. and Kuller, L. (2005). Combined postmenopausal hormone therapy and cardiovascular disease: toward resolving the discrepancy between observational studies and the women's health initiative clinical trial, *American Journal of Epidemiology* **162**: 404–414.

Richardson, T. S., Robins, J. M. and Wang, L. (2017). On modeling and estimation for the relative risk and risk difference, *Journal of the American Statistical Association* **112**: 1121–1130.

Robins, J. M. (1994). Correcting for non-compliance in randomized trials using structural nested mean models, *Communications in Statistics-Theory and Methods* **23**: 2379–2412.

Rothwell, P. M. (2005). Subgroup analysis in randomised controlled trials: importance, indications, and interpretation, *The Lancet* **365**: 176–186.

Rothwell, P. M., Mehta, Z., Howard, S. C., Gutnikov, S. A. and Warlow, C. P. (2005). From subgroups to individuals: general principles and the example of carotid endarterectomy, *The Lancet* **365**: 256–265.

Rotnitzky, A., Smucler, E. and Robins, J. M. (2019). Characterization of parameters with a mixed bias property, *arXiv preprint arXiv:1904.03725* .

Rubin, D. B. (1974). Estimating causal effects of treatments in randomized and nonrandomized studies, *Journal of Educational Psychology* **66**: 688–701.

Rudolph, K. E. and van der Laan, M. J. (2017). Robust estimation of encouragement design intervention effects transported across sites, *Journal of the Royal Statistical Society: Series B (Statistical Methodology)* **79**: 1509–1525.

Shao, J. (1994). Bootstrap sample size in nonregular cases, *Proceedings of the American Mathematical Society* **122**: 1251–1262.

Sherman, R. E., Anderson, S. A., Dal Pan, G. J., Gray, G. W., Gross, T., Hunter, N. L., LaVange, L., Marinac-Dabic, D., Marks, P. W., Robb, M. A., Shuren, J., Temple, R., Woodcock, J., Yue, L. and Califf, R. (2016). Real-world evidence—what is it and what can it tell us, *New England Journal of Medicine* **375**: 2293–2297.

Shi, C., Song, R. and Lu, W. (2016). Robust learning for optimal treatment decision with np-dimensionality, *Electronic Journal of Statistics* **10**: 2894–2921.

Sobel, M., Madigan, D. and Wang, W. (2017). Causal inference for meta-analysis and multi-level data structures, with application to randomized studies of vioxx, *Psychometrika* **82**: 459–474.

Staiger, D. and Stock, J. H. (1997). Instrumental variables regression with weak instruments, *Econometrica* **65**: 557–586.

Stefanski, L. A. and Boos, D. D. (2002). The calculus of m-estimation, *The American Statistician* **56**: 29–38.

Strauss, G. M., Herndon, J. E., II, M. A. M., Johnstone, D. W., Johnson, E. A., Harpole, D. H., Gillenwater, H. H., Watson, D. M., Sugarbaker, D. J. and Schilsky, R. L. (2008). Adjuvant paclitaxel plus carboplatin compared with observation in stage IB non–small-cell lung cancer: CALGB 9633 with the Cancer and Leukemia Group B, Radiation Therapy Oncology Group, and North Central Cancer Treatment Group Study Groups, *Journal of Clinical Oncology* **26**: 5043–5051.

Stuart, E. A., Cole, S. R., Bradshaw, C. P. and Leaf, P. J. (2011). The use of propensity scores to assess the generalizability of results from randomized trials, *Journal of the Royal Statistical Society: Series A (Statistics in Society)* **174**: 369–386.

Tallis, G. (1963). Elliptical and radial truncation in normal populations, *The Annals of Mathematical Statistics* **34**: 940–944.

Tian, L., Alizadeh, A., Gentles, A. and Tibshirani, R. (2014). A simple method for estimating interactions between a treatment and a large number of covariates, *Journal of the American Statistical Association* **109**: 1517–1532.

Toyoda, T. and Wallace, T. D. (1979). Pre-testing on part of the data, *Journal of Econometrics* **10**: 119–123.

US Food and Drug Administration (2019). Rare diseases: Natural history studies for drug development, *https:// www. fda. gov/ media/ 122425/ downl oad (accessed 1 May 2022)* .

van der Vaart, A. W. (2000). *Asymptotic Statistics*, Cambridge University Press, Cambridge, MA.

van der Vaart, A. W. and Wellner, J. A. (1996). *Weak Convergence and Emprical Processes: With Applications to Statistics*, New York: Springer.

Verde, P. E. and Ohmann, C. (2015). Combining randomized and non-randomized evidence in clinical research: a review of methods and applications, *Research Synthesis Methods* **6**: 45–62.

Wu, L. and Yang, S. (2021). Transfer learning of individualized treatment rules from experimental to real-world data, *arXiv preprint arXiv:2108.08415* .

Wu, L. and Yang, S. (2022). Integrative r-learner of heterogeneous treatment effects combining experimental and observational studies, *Proceedings of Machine Learning Research*, Vol. 140, pp. 1–S5.

Yang, S. and Ding, P. (2018). Asymptotic inference of causal effects with observational studies trimmed by the estimated propensity scores, *Biometrika* **105**: 487–493.

Yang, S. and Kim, J. K. (2019). Integration of survey data and big observational data for finite population inference using mass imputation, *International Statistical Review* p. revision.

Yang, S. and Kim, J. K. (2020). Statistical data integration in survey sampling: A review, *Japanese Journal of Statistics and Data Science* **3**: 625–650.

Yang, S., Kim, J. K. and Song, R. (2019). Doubly robust inference when combining probability and non-probability samples with high-dimensional data, *Journal of the Royal Statistical Society, Series B* p. doi:10.1111/rssb.12354.

Zhao, Y.-Q., Zeng, D., Tangen, C. M. and Leblanc, M. L. (2019). Robustifying trial-derived optimal treatment rules for a target population, *Electronic Journal of Statistics* **13**: 1717–1743.

Supplementary materials for "Elastic integrative analysis of randomized trial and real-world data for treatment heterogeneity estimation"

by Yang, Gao, Zeng, and Wang

Section S1 provides technical details and proofs for (rate) doubly robust estimation.
Section S2 provides technical details for the test and elastic estimator.
Section S3 provides technical details for inference.
Section S4 provides additional simulation results and studies.

S1 Technical details for rate doubly robust estimation

S1.1 Regularity conditions for rate double robustness

Recall that $\mathbb{P}_N$ denotes the empirical measure over the combined RT and RW data; i.e., $\mathbb{P}_N h(V) = N^{-1}\sum_{i\in\mathcal{A}\cup\mathcal{B}} h(V_i)$. Also, $\mathbb{P}\{h(V)\} = \int h(V)\mathrm{d}\mathbb{P}$ denotes the expectation of $h(V)$ over the data generative distribution.

Assumption S1. The following regularity conditions hold:

a) $S_{\psi_0}(V)$ belongs to a Donsker class (van der Vaart and Wellner, 1996);

b) $S_\psi(V)$ is differentiable in ψ, and $\mathbb{E}\{\partial S_{\psi_0}(V)/\partial\psi^{\mathrm{T}}\}$ exists and is invertible;

c) there exists a constant C such that $|\partial\tau_{\psi_0}(X)/\partial\psi| \le C$ and $|\left\{\sigma_\delta^2(X)\right\}^{-1}| \le C$ almost surely.

S1.2 Proof of Theorem 1

Proof. Under Assumption S1, by the standard Taylor expansion, we have

$$N^{1/2}\left(\widehat{\psi}_{\mathrm{eff}} - \psi_0\right) = \left[\mathbb{E}\{\partial S_{\psi_0}(V)/\partial\psi^{\mathrm{T}}\}\right]^{-1} N^{1/2}\mathbb{P}_N\widehat{S}_{\psi_0}(V) + o_{\mathbb{P}}(N^{-1/2}). \tag{S1}$$

Moreover, we have

$$\begin{aligned}\mathbb{P}_N\widehat{S}_{\psi_0}(V) &= (\mathbb{P}_N - \mathbb{P})\widehat{S}_{\psi_0}(V) + \mathbb{P}\widehat{S}_{\psi_0}(V)\\ &= (\mathbb{P}_N - \mathbb{P})S_{\psi_0}(V) + \mathbb{P}\widehat{S}_{\psi_0}(V) + o_{\mathbb{P}}(N^{-1/2})\\ &= \mathbb{P}_N S_{\psi_0}(V) + \mathbb{P}\widehat{S}_{\psi_0}(V) + o_{\mathbb{P}}(N^{-1/2}),\end{aligned} \tag{S2}$$

where the third equality follows because of $\mathbb{P}S_{\psi_0}(V) = 0$ by Assumption 3.

We now show that the second term in (S2), $\mathbb{P}\widehat{S}_{\psi_0}(V)$, is a small order term. We write

$$\mathbb{P}\widehat{S}_{\psi_0}(V) = \mathbb{P}\left[\left\{\frac{\partial \tau_{\psi_0}(X)}{\partial \psi}\right\}\left\{\sigma_\delta^2(X)\right\}^{-1}\left\{\mu_\delta(X) - \widehat{\mu}_\delta(X)\right\}\left\{e_\delta(X) - \widehat{e}_\delta(X)\right\}\right]. \tag{S3}$$

By trial design, the propensity score of treatment is known; i.e., $\widehat{e}_1(X) = e_1(X)$. Therefore, we have

$$\mathbb{P}\left[\delta\left\{\frac{\partial \tau_{\psi_0}(X)}{\partial \psi}\right\}\left\{\sigma_1^2(X)\right\}^{-1}\left\{\mu_1(X) - \widehat{\mu}_1(X)\right\}\left\{e_1(X) - \widehat{e}_1(X)\right\}\right] = 0.$$

Then, (S3) becomes

$$\mathbb{P}\widehat{S}_{\psi_0}(V) = \mathbb{P}\left[(1-\delta)\left\{\frac{\partial \tau_{\psi_0}(X)}{\partial \psi}\right\}\left\{\sigma_0^2(X)\right\}^{-1}\left\{\mu_0(X) - \widehat{\mu}_0(X)\right\}\left\{e_0(X) - \widehat{e}_0(X)\right\}\right].$$

By the Cauchy-Schwarz inequality, $|\mathbb{P}\widehat{S}_{\psi_0}(V)|$ is bounded by

$$C^2\|\mu_0(X) - \widehat{\mu}_0(X)\| \times \|e_0(X) - \widehat{e}_0(X)\|. \tag{S4}$$

Under the assumptions in Theorem 1, the product (S4) is $o_{\mathbb{P}}(N^{-1/2})$. Therefore, $\mathbb{P}\widehat{S}_{\psi_0}(V)$ in (S2) is asymptotically negligible. Therefore, (S2) becomes

$$\mathbb{P}_N\widehat{S}_{\psi_0}(V) = o_{\mathbb{P}}(N^{-1/2}). \tag{S5}$$

Combining (S1), (S2) and (S5), the results in Theorem 1 follow. □

S1.3 Sieves estimation

We illustrate Theorem 1 by the method of sieves. For simplicity, we consider the power series, although our discussion extends to general sieve basis functions such as Fourier series, splines, wavelets, and artificial neural networks (see, e.g., Chen, 2007). Let d_X be the dimension of X. For a d_X-vector of non-negative integers $\kappa = (\kappa_1, \ldots, \kappa_{d_X})$, let $|\kappa| = \sum_{l=1}^{d_X}\kappa_l$ and $X^\kappa = \prod_{l=1}^{d_X} X_l^{\kappa_l}$. Define a series $\{\kappa(k) : k = 1, 2, \ldots\}$ for all distinct vectors of κ such that $|\kappa(k)| \leq |\kappa(k+1)|$. Based on this series, we consider a K-vector $g(X) = \{g_1(X), \ldots, g_K(X)\}^\top = \{X^{\kappa(1)}, \ldots, X^{\kappa(K)}\}^\top$.

To accommodate different type of variables, we approximate $e_0(X)$ and $\mu_\delta(X)$ by the generalized sieves functions

$$\text{expit}\left\{\alpha^{*\mathrm{T}} g(X)\right\}, \qquad h\left\{\eta_\delta^{*\top} g(X)\right\}, \tag{S6}$$

where expit$(\cdot)$ is the inverse of logit$(\cdot)$, $h(\cdot)$ is a certain link function, e.g., for a continuous outcome, $h(\cdot)$ is an identity function, and for a binary outcome, $h(\cdot)$ is an expit function, and

$$\begin{aligned}
\alpha^* &= \arg\min_\alpha \mathbb{E}[e_0(X) - \text{expit}\{\alpha^{\mathrm{T}} g(X)\}]^2, \\
\eta_\delta^* &= \arg\min_\eta \mathbb{E}\left[\mu_\delta(X) - h\{\eta_\delta^{\mathrm{T}} g(X)\}\right]^2.
\end{aligned}$$

We provide the regularity conditions below, under which the sieves estimators satisfy the conditions in Theorem 1, and therefore $\widehat{\psi}_{\text{eff}}$ enjoys the properties in Theorem 1.

Assumption S2. The following regularity conditions hold:

a) the density of X, $f(X)$, is bounded above and below away from 0 on $\mathcal{X}$;

b) $\mathbb{E}[\{Y(a)\}^2] < \infty$, for $a = 0, 1$;

c) $e_0(X)$ is s_1-times continuously differentiable, and $\mu_\delta(X)$ is s_2-times continuously differentiable; let $s_0 = \min(s_1, s_2)$, which satisfies that $s_0 \geq 3d_X$;

d) there exist constant l and u such that $l \leq \rho_{\min}\{g(X)^\top g(X)\} \leq \rho_{\max}\{g(X)^\top g(X)\} \leq u$ almost surely, where $\rho_{\min}(M)$ and $\rho_{\max}(M)$ denote the minimum and maximum eigenvalues of a matrix;

e) $K = O\left(n^{\frac{d_X}{s_0 - d_X}}\right)$.

Under certain regularity conditions, we show that the method of sieves allows flexible models for $e_0(X)$ and $\mu_\delta(X)$ and also satisfies Assumption 3. Let $\mathcal{X} \subseteq \mathbb{R}^{d_X}$ be the support of X. Assume that $\mathcal{X}$ is a Cartesian product of compact intervals, i.e. $\mathcal{X} = \prod_{j=1}^{p} [l_j, u_j]$, $l_j, u_j \in \mathbb{R}$.

Following Newey (1997), under Assumption S2, the bounds for the deterministic differences between the true functions and the sieves approximations are

$$\begin{aligned} \sup_{x \in \mathcal{X}} |e_0(x) - \operatorname{expit}\{\alpha^{*\mathrm{T}} g(x)\}| &= O\left\{K^{1-s_1/(2d_X)}\right\}, \\ \sup_{x \in \mathcal{X}} |\mu_\delta(x) - h\{\eta_\delta^{*\mathrm{T}} g(x)\}| &= O\left\{K^{1-s_2/(2d_X)}\right\}. \end{aligned} \tag{S7}$$

On the one hand, given (S7), the approximation errors can be made sufficiently small if the number of basis functions K is large. On the other hand, in order to control the variance of the sieves estimators, K should increase slowly with the sample size n. Concretely, under regularity conditions, $\widehat{\alpha} - \alpha^* = O_{\mathbb{P}}(K/n)$ and $\widehat{\eta}_\delta - \eta_\delta^* = O_{\mathbb{P}}(K/n)$. Therefore, the bias of the sieves approximation for $e_0(X)$ is $O_{\mathbb{P}}\left\{K^{1-s_1/(2d_X)}\right\}$ and the variance is $O_{\mathbb{P}}\left(K/n\right)$. Similarly, the bias of the sieves approximation for $\mu_\delta(X)$ is $O_{\mathbb{P}}\left\{K^{1-s_2/(2d_X)}\right\}$ and the variance is $O_{\mathbb{P}}\left(K/n\right)$. With $K = O\left\{n^{d_X/(s_0-d_X)}\right\}$ in Assumption S2 (v), it balances the squared bias and variance with both $O_{\mathbb{P}}\left\{n^{(2d_X-s_0)/(s_0-d_X)}\right\}$. Then under Assumption S2 (iii), Assumption 3 holds.

S2 Technical details for the test and elastic estimator

We introduce additional notation. For convenience, Table S1 summarizes additional notation and their properties for references.

To gauge the strength of the evidence, we characterize the asymptotic distribution of $n^{-1/2} \sum_{i \in \mathcal{B}} \widehat{S}_{\mathrm{rw},\widehat{\psi}_{\mathrm{rt}}}(V_i)$ under H_0, H_a and $\mathrm{H}_{a,n}$. Toward this end, we introduce two random variables

$$\begin{gathered} \mathcal{Z}_{\mathrm{rt}} \sim \mathrm{Normal}(0, \mathcal{I}_{\mathrm{rt}}), \quad \mathcal{Z}_{\mathrm{rw}} \sim \mathrm{Normal}(\mu_{\mathrm{rw}}, \mathcal{I}_{\mathrm{rw}}), \\ \mathcal{I}_{\mathrm{rt}} = \mathbb{E}\{S_{\mathrm{rt},\psi_0}(V)^{\otimes 2} \mid \delta = 1\}, \quad \mathcal{I}_{\mathrm{rw}} = \mathbb{E}\{S_{\mathrm{rw},\psi_0}(V)^{\otimes 2} \mid \delta = 0\}. \end{gathered}$$

Under H_0, $\mu_{\mathrm{rw}} = 0$; under H_a, $\mu_{\mathrm{rw}} = \infty$; and under $\mathrm{H}_{a,n}$, $\mu_{\mathrm{rw}} = \eta$. By the generalized information equality, we also have $\mathcal{I}_{\mathrm{rt}} = \mathbb{E}\{\partial S_{\mathrm{rt},\psi_0}(V)/\partial\psi \mid \delta = 1\}$ and $\mathcal{I}_{\mathrm{rw}} = \mathbb{E}\{\partial S_{\mathrm{rw},\psi_0}(V)/\partial\psi \mid \delta = 0\}$. Based on $\mathcal{Z}_{\mathrm{rt}}$ and $\mathcal{Z}_{\mathrm{rw}}$, by central limit theorem, we have

Table S1: Notation and properties

Notation	Definition	Property
$\mathcal{I}_{\text{rw}}$	$\mathbb{E}\{S_{\text{rw},\psi_0}(V)^{\otimes 2} \mid \delta = 0\}$	
$\mathcal{I}_{\text{rt}}$	$\mathbb{E}\{S_{\text{rt},\psi_0}(V)^{\otimes 2} \mid \delta = 1\}$	
Γ	$\mathcal{I}_{\text{rt}}^{-1}\mathcal{I}_{\text{rw}}\rho^{-1/2}$	
Σ_{SS}	$\Gamma^{\text{T}}\mathcal{I}_{\text{rt}}\Gamma + \mathcal{I}_{\text{rw}}$	
V_{rt}	$(\rho\mathcal{I}_{\text{rt}})^{-1}$	
V_{eff}	$(\rho\mathcal{I}_{\text{rt}} + \mathcal{I}_{\text{rw}})^{-1}$	
$V_{\text{rt-eff}}$	$V_{\text{rt}} - V_{\text{eff}}$	$V_{\text{rt-eff}}\Sigma_{SS}^{-1} = V_{\text{eff}}^2$, $V_{\text{rt-eff}} = V_{\text{eff}}\Sigma_{SS}V_{\text{eff}}$
$\mathcal{Z}_{\text{rw}}$	$\text{Normal}(\mu_{\text{rw}}, \mathcal{I}_{\text{rw}})$	
$\mathcal{Z}_{\text{rt}}$	$\text{Normal}(0, \mathcal{I}_{\text{rt}})$	
Under H_0, $\mu_{\text{rw}} = 0$; under H_a, $\mu_{\text{rw}} = \infty$; and under $\text{H}_{a,n}$, $\mu_{\text{rw}} = \eta$.		
$\mathcal{Z}_1$	$\Sigma_{SS}^{-1/2}(\mathcal{Z}_{\text{rw}} - \Gamma^{\text{T}}\mathcal{Z}_{\text{rt}})$	$\sim \text{Normal}(\Sigma_{SS}^{-1/2}\mu_{\text{rw}}, I_{p\times p})$
$\mathcal{Z}_2$	$V_{\text{eff}}^{1/2}(\mathcal{Z}_{\text{rw}} + \rho^{1/2}\mathcal{Z}_{\text{rt}})$	$\sim \text{Normal}(V_{\text{eff}}^{1/2}\mu_{\text{rw}}, I_{p\times p})$
	$\mu_1 = \Sigma_{SS}^{-1/2}\eta$ and $\mu_2 = V_{\text{eff}}^{1/2}\eta$	
Definition	Representation using $\mathcal{Z}_{\text{rw}}$ and $\mathcal{Z}_{\text{rt}}$	Orthogonal representation using $\mathcal{Z}_1$ and $\mathcal{Z}_2$
$T_\infty(\mathcal{Z}_{\text{rt}}, \mathcal{Z}_{\text{rw}})$	$(\mathcal{Z}_{\text{rw}} - \Gamma^{\text{T}}\mathcal{Z}_{\text{rt}})^{\text{T}}\Sigma_{SS}^{-1}(\mathcal{Z}_{\text{rw}} - \Gamma^{\text{T}}\mathcal{Z}_{\text{rt}})$	$\mathcal{Z}_1^{\text{T}}\mathcal{Z}_1$
$\mathcal{N}_{\text{rt}}(\mathcal{Z}_{\text{rt}})$	$-(\rho\mathcal{I}_{\text{rt}})^{-1}(\rho^{1/2}\mathcal{Z}_{\text{rt}})$	$V_{\text{rt-eff}}^{1/2}\mathcal{Z}_1 - V_{\text{eff}}^{1/2}\mathcal{Z}_2$
bias	0	$(V_{\text{rt-eff}}^{1/2}\Sigma_{SS}^{-1/2} - V_{\text{eff}})\eta = 0$
var	$(\rho\mathcal{I}_{\text{rt}})^{-1}$	$V_{\text{rt-eff}} + V_{\text{eff}} = V_{\text{rt}}$
$\mathcal{N}_{\text{eff}}(\mathcal{Z}_{\text{rt}}, \mathcal{Z}_{\text{rw}})$	$-(\rho\mathcal{I}_{\text{rt}} + \mathcal{I}_{\text{rw}})^{-1}(\rho^{1/2}\mathcal{Z}_{\text{rt}} + \mathcal{Z}_{\text{rw}})$	$-V_{\text{eff}}^{1/2}\mathcal{Z}_2$
bias	$-(\rho\mathcal{I}_{\text{rt}} + \mathcal{I}_{\text{rw}})^{-1}\mu_{\text{rw}}$	$-V_{\text{eff}}\eta$
var	$(\rho\mathcal{I}_{\text{rt}} + \mathcal{I}_{\text{rw}})^{-1}$	V_{eff}

$$m^{-1/2}\sum_{i\in\mathcal{A}} S_{\text{rt},\psi_0}(V_i) \dot{\sim} \mathcal{Z}_{\text{rt}},\ n^{-1/2}\sum_{i\in\mathcal{B}} S_{\text{rw},\psi_0}(V_i) \dot{\sim} \mathcal{Z}_{\text{rw}}.$$

Using $\mathcal{Z}_{\text{rt}}$ and $\mathcal{Z}_{\text{rw}}$ is also helpful to characterize the asymptotic distributions of $\widehat{\psi}_{\text{rt}}$, $\widehat{\psi}_{\text{eff}}$, and our proposed estimator in the later section. Building on the asymptotic properties of the score functions, we have

$$n^{1/2}(\widehat{\psi}_{\text{rt}} - \psi_0) \dot{\sim} \mathcal{N}_{\text{rt}},\quad n^{1/2}(\widehat{\psi}_{\text{eff}} - \psi_0) \dot{\sim} \mathcal{N}_{\text{eff}}, \tag{S8}$$

where

$$\mathcal{N}_{\text{rt}} = -(\rho\mathcal{I}_{\text{rt}})^{-1}(\rho^{1/2}\mathcal{Z}_{\text{rt}}),\quad \mathcal{N}_{\text{eff}} = -(\rho\mathcal{I}_{\text{rt}} + \mathcal{I}_{\text{rw}})^{-1}(\rho^{1/2}\mathcal{Z}_{\text{rt}} + \mathcal{Z}_{\text{rw}}). \tag{S9}$$

The results in (S8) facilitate an easy comparison of $\widehat{\psi}_{\text{rt}}$ and $\widehat{\psi}_{\text{eff}}$. Under the idealistic assumption, $\mathbb{V}_a\{n^{1/2}(\widehat{\psi}_{\text{rt}} - \psi_0)\} = V_{\text{rt}} = (\rho\mathcal{I}_{\text{rt}})^{-1}$, and $\mathbb{V}_a\{n^{1/2}(\widehat{\psi}_{\text{eff}} - \psi_0)\} = V_{\text{eff}} = (\rho\mathcal{I}_{\text{rt}} + \mathcal{I}_{\text{rw}})^{-1}$, where ρ can be viewed as the relative sample size of the RT data compared with the RW data. It is clear that the difference between V_{rt} and V_{eff} is $V_{\text{rt-eff}} = (\rho\mathcal{I}_{\text{rt}})^{-1} - (\rho\mathcal{I}_{\text{rt}} + \mathcal{I}_{\text{rw}})^{-1} > 0$ and $\widehat{\psi}_{\text{eff}}$ gains efficiency by using the additional information in the RW data.

We characterize the asymptotic distribution of $n^{-1/2}\sum_{i\in\mathcal{B}}\widehat{S}_{\text{rw},\widehat{\psi}_{\text{rt}}}(V_i)$ using $\mathcal{Z}_{\text{rt}}$ and $\mathcal{Z}_{\text{rw}}$, which is the building block to constructing the test statistic.

Proposition S1. Suppose assumptions in Theorem 1 hold except that Assumption 2 may be violated. Let $\Gamma = \mathcal{I}_{\text{rt}}^{-1}\mathcal{I}_{\text{rw}}\rho^{-1/2}$. Then,

$$n^{-1/2}\sum_{i\in\mathcal{B}}\widehat{S}_{\text{rw},\widehat{\psi}_{\text{rt}}}(V_i) \dot{\sim} \mathcal{Z}_{\text{rw}} - \Gamma^{\text{T}}\mathcal{Z}_{\text{rt}}. \tag{S10}$$

a) Under H_0, (S10) is a normal distribution with mean 0 and variance Σ_{SS}.

b) Under H_a, (S10) is $\pm\infty$.

c) Under $\text{H}_{a,n}$, (S10) is a normal distribution with mean η and variance Σ_{SS}.

In Proposition S1, because of the intrinsic connection between $\text{H}_{a,n}$ and the other two hypotheses, the result in c) reduces to that in a) by considering $\eta = 0$ and to that in b) by considering $\eta = \pm\infty$.

Proposition S2. Suppose assumptions in Theorem 1 hold except that Assumption 2 may be violated.

a) Under H_0, we have $T \dot{\sim} \chi_p^2$, a Chi-square distribution with degrees of freedom p, as $n \to \infty$.

b) Under H_a, we have $T \to \infty$, almost surely, as $n \to \infty$.

c) Under $\text{H}_{a,n}$, we have $T \dot{\sim} \chi_p^2(\lambda)$, a non-central Chi-square distribution with degrees of freedom p and non-centrality parameter $\lambda = \eta^{\text{T}}\Sigma_{SS}^{-1}\eta$, as $n \to \infty$.

Not surprisingly, in Theorem S2, $\chi_p^2(\lambda)$ in c) becomes χ_p^2 in a) by considering $\eta = 0$ and to ∞ in b) by considering $\eta = \pm\infty$.

Recall that the asymptotic distributions of $\widehat{\psi}_{\text{rt}}$ and $\widehat{\psi}_{\text{eff}}$ can be easily represented by $\mathcal{N}_{\text{rt}}$ and $\mathcal{N}_{\text{eff}}$ as in (S8). However, the distributions of $\widehat{\psi}_{\text{rt}} \mid (T \geq c_\gamma)$ and $\widehat{\psi}_{\text{eff}} \mid (T < c_\gamma)$ are those constrained to the acceptance and rejection regions of the test. Below, we characterize these asymptotic distributions, taking into account that the estimators and the test may be correlated asymptotically.

Let the asymptotic distribution of T be represented by

$$T_\infty = (\mathcal{Z}_{\text{rw}} - \Gamma^{\text{T}}\mathcal{Z}_{\text{rt}})^{\text{T}}\Sigma_{SS}^{-1}(\mathcal{Z}_{\text{rw}} - \Gamma^{\text{T}}\mathcal{Z}_{\text{rt}}). \tag{S11}$$

By (S17), asymptotically, the event $T < c_\gamma$ corresponds to $T_\infty < c_\gamma$ and the event $T \geq c_\gamma$ corresponds to $T_\infty \geq c_\gamma$. We show in the supplementary material that

$$\widehat{\psi}_{\text{rt}} \mid (T \geq c_\gamma) \quad \dot{\sim} \quad \mathcal{N}_{\text{rt}} \mid (T_\infty \geq c_\gamma), \tag{S12}$$

$$\widehat{\psi}_{\text{eff}} \mid (T < c_\gamma) \quad \dot{\sim} \quad \mathcal{N}_{\text{eff}} \mid (T_\infty < c_\gamma). \tag{S13}$$

The limiting distributions in (S12) and (S13) are multivariate normal distributions with ellipsoid truncation (Tallis, 1963). Specifically, (S12) is the multivariate normal distribution $\mathcal{N}_{\text{rt}}$ outside the boundary of the ellipsoid $T_\infty = c_\gamma$, and (S13) is the multivariate normal distribution $\mathcal{N}_{\text{eff}}$ inside the boundary of the ellipsoid $T_\infty = c_\gamma$.

Based on (S11), it is insightful to recognize that T_∞ is fully characterized by $\mathcal{Z}_{\text{rw}} - \Gamma^{\text{T}}\mathcal{Z}_{\text{rt}}$. We introduce two normal random vectors

$$\mathcal{Z}_1 = \Sigma_{SS}^{-1/2}(\mathcal{Z}_{\text{rw}} - \Gamma^{\text{T}}\mathcal{Z}_{\text{rt}}), \quad \mathcal{Z}_2 = V_{\text{eff}}^{1/2}(\mathcal{Z}_{\text{rw}} + \rho^{1/2}\mathcal{Z}_{\text{rt}}),$$

which are multivariate normal distributions with means $\Sigma_{SS}^{-1/2}\mu_{\rm rw}$ and $V_{\rm eff}^{1/2}\mu_{\rm rw}$, respectively, and covariance $I_{p\times p}$. Under H_0, it is easy to verify that the covariance of $\mathcal{Z}_1$ and $\mathcal{Z}_2$ is zero. Because uncorrelated normal random vectors are independent, $\mathcal{Z}_1$ and $\mathcal{Z}_2$ are independent. Similarly, we can show that under H_a and $\mathrm{H}_{a,n}$, $\mathcal{Z}_1$ and $\mathcal{Z}_2$ are independent. Translating the asymptotic distributions (S12) and (S13) into the ones using $\mathcal{Z}_1$ and $\mathcal{Z}_2$ makes the characterization easier. First, T_∞ is equivalent to $\mathcal{Z}_1^{\rm T}\mathcal{Z}_1$.

S2.1 Proof of Proposition S2

Proof. Because we construct the test statistic T based on $\sum_{i\in\mathcal{B}}\widehat{S}_{{\rm rw},\widehat{\psi}_{\rm rt}}(V_i)$, where $\widehat{\psi}_{\rm rt}$ satisfies $\sum_{i\in\mathcal{A}}\widehat{S}_{{\rm rt},\widehat{\psi}_{\rm rt}}(V_i)=0$, we first investigate the statistical properties of $\sum_{i\in\mathcal{A}}\widehat{S}_{{\rm rt},\widehat{\psi}_{\rm rt}}(V_i)$ and $\sum_{i\in\mathcal{B}}\widehat{S}_{{\rm rw},\widehat{\psi}_{\rm rt}}(V_i)$, both properly scaled.

By the Taylor expansion, we have

$$\begin{aligned} m^{-1/2}\sum_{i\in\mathcal{A}}\widehat{S}_{{\rm rt},\widehat{\psi}_{\rm rt}}(V_i) &= m^{-1/2}\sum_{i\in\mathcal{A}}S_{{\rm rt},\psi_0}(V_i) \\ &\quad +m^{-1/2}\mathbb{E}\left\{\sum_{i\in\mathcal{A}}\frac{\partial S_{{\rm rt},\psi_0}(V_i)}{\partial\psi^{\rm T}}\right\}(\widehat{\psi}_{\rm rt}-\psi_0)+o_{\mathbb{P}}(1) \\ &= m^{-1/2}\sum_{i\in\mathcal{A}}S_{{\rm rt},\psi_0}(V_i)+\mathcal{I}_{\rm rt}\left\{m^{1/2}(\widehat{\psi}_{\rm rt}-\psi_0)\right\}+o_{\mathbb{P}}(1), \end{aligned}$$

where $o_{\mathbb{P}}(1)$ follows by a similar argument for (S5). Then, we have

$$m^{1/2}(\widehat{\psi}_{\rm rt}-\psi_0)=-(\mathcal{I}_{\rm rt})^{-1}m^{-1/2}\sum_{i\in\mathcal{A}}S_{{\rm rt},\psi_0}(V_i)+o_{\mathbb{P}}(1). \tag{S14}$$

By the Taylor expansion, we have

$$\begin{aligned} n^{-1/2}\sum_{i\in\mathcal{B}}\widehat{S}_{{\rm rw},\widehat{\psi}_{\rm rt}}(V_i) &= n^{-1/2}\sum_{i\in\mathcal{B}}S_{{\rm rw},\psi_0}(V_i) \\ &\quad +n^{-1/2}\mathbb{E}\left\{\sum_{i\in\mathcal{B}}\frac{\partial S_{{\rm rw},\psi_0}(V_i)}{\partial\psi^{\rm T}}\right\}(\widehat{\psi}_{\rm rt}-\psi_0)+o_{\mathbb{P}}(1) \\ &= n^{-1/2}\sum_{i\in\mathcal{B}}S_{{\rm rw},\psi_0}(V_i)+\mathcal{I}_{\rm rw}\left\{n^{1/2}(\widehat{\psi}_{\rm rt}-\psi_0)\right\}+o_{\mathbb{P}}(1), \end{aligned} \tag{S15}$$

where $o_{\mathbb{P}}(1)$ follows by a similar argument for (S5).

Combining (S14) and (S15) leads to

$$\begin{aligned} n^{-1/2}\sum_{i\in\mathcal{B}}\widehat{S}_{{\rm rw},\widehat{\psi}_{\rm rt}}(V_i) &= \left\{n^{-1/2}\sum_{i\in\mathcal{B}}S_{{\rm rw},\psi_0}(V_i)\right\} \\ &\quad -\mathcal{I}_{\rm rw}(\mathcal{I}_{\rm rt})^{-1}\left(\frac{n}{m}\right)^{1/2}\left\{m^{-1/2}\sum_{i\in\mathcal{A}}S_{{\rm rt},\psi_0}(V_i)\right\}+o_{\mathbb{P}}(1)\dot{\sim}\mathcal{Z}_{\rm rw}-\Gamma^{\rm T}\mathcal{Z}_{\rm rt}. \end{aligned} \tag{S16}$$

Specifically, $\mathcal{Z}_{\rm rw}-\Gamma^{\rm T}\mathcal{Z}_{\rm rt}$ follows Normal$(0,\Sigma_{SS})$, where $\Sigma_{SS}=\mathbb{V}(\mathcal{Z}_{\rm rw}-\Gamma^{\rm T}\mathcal{Z}_{\rm rt})=\mathcal{I}_{\rm rw}+\Gamma^{\rm T}\mathcal{I}_{\rm rt}\Gamma$.

Therefore, it follows that

$$T \dot{\sim} (\mathcal{Z}_{\mathrm{rw}} - \Gamma^{\mathrm{T}}\mathcal{Z}_{\mathrm{rt}})\Sigma_{SS}^{-1}(\mathcal{Z}_{\mathrm{rw}} - \Gamma^{\mathrm{T}}\mathcal{Z}_{\mathrm{rt}}) \sim \chi_p^2. \tag{S17}$$

□

S2.2 Asymptotic distribution of an estimator given the test constraint

We first provide a useful proposition.

Proposition S3. Suppose the assumptions in Theorem S2 holds. For $p \times p$ matrices A and B,

$$A^{\mathrm{T}}\left\{n^{-1/2}\sum_{i\in\mathcal{A}} S_{\psi_0}(V_i)\right\} + B^{\mathrm{T}}\left\{m^{-1/2}\sum_{i\in\mathcal{B}} S_{\psi_0}(V_i)\right\} \Bigg| (T < c_\gamma)$$
$$\dot{\sim} A^{\mathrm{T}}\mathcal{Z}_{\mathrm{rt}} + B^{\mathrm{T}}\mathcal{Z}_{\mathrm{rw}} \mid (T_\infty < c_\gamma), \tag{S18}$$

and

$$A^{\mathrm{T}}\left\{n^{-1/2}\sum_{i\in\mathcal{A}} S_{\psi_0}(V_i)\right\} + B^{\mathrm{T}}\left\{m^{-1/2}\sum_{i\in\mathcal{B}} S_{\psi_0}(V_i)\right\} \Bigg| (T \geq c_\gamma)$$
$$\dot{\sim} A^{\mathrm{T}}\mathcal{Z}_{\mathrm{rt}} + B^{\mathrm{T}}\mathcal{Z}_{\mathrm{rw}} \mid (T_\infty \geq c_\gamma). \tag{S19}$$

Proof. Denote $Q_n = A^{\mathrm{T}}\left\{n^{-1/2}\sum_{i\in\mathcal{A}} S_{\psi_0}(V_i)\right\} + B^{\mathrm{T}}\left\{m^{-1/2}\sum_{i\in\mathcal{B}} S_{\psi_0}(V_i)\right\}$ and $Q = A^{\mathrm{T}}\mathcal{Z}_{\mathrm{rt}} + B^{\mathrm{T}}\mathcal{Z}_{\mathrm{rw}}$. By Theorem S2, we have

$$\begin{pmatrix} Q_n \\ T \end{pmatrix} \dot{\sim} \begin{pmatrix} Q \\ T_\infty \end{pmatrix}.$$

By the continuous mapping theorem, we have

$$\begin{pmatrix} Q_n \\ \mathbf{1}(T < c_\gamma) \end{pmatrix} \dot{\sim} \begin{pmatrix} Q \\ \mathbf{1}(T_\infty < c_\gamma) \end{pmatrix}.$$

By the Portmanteau Theorem, for all bounded continuous functions $h : \mathbb{R}^p \mapsto \mathbb{R}$, we have

$$\mathbb{E}\{h(Q_n)\mathbf{1}(T < c_\gamma)\} \to \mathbb{E}\{h(Q)\mathbf{1}(T_\infty < c_\gamma)\}.$$

For all bounded continuous functions $h : \mathbb{R}^p \mapsto \mathbb{R}$, we have

$$\mathbb{E}\{h(Q_n) \mid \mathbf{1}(T < c_\gamma)\} = \frac{\mathbb{E}\{h(Q_n)\mathbf{1}(T < c_\gamma)\}}{\mathbb{P}(T < c_\gamma)}$$
$$\to \frac{\mathbb{E}\{h(Q)\mathbf{1}(T_\infty < c_\gamma)\}}{\mathbb{P}\{\mathbf{1}(T_\infty < c_\gamma)\}} = \mathbb{E}\{h(Q) \mid \mathbf{1}(T_\infty < c_\gamma)\},$$

as $n \to \infty$. Applying the Portmanteau Theorem, $Q_n \mid \mathbf{1}(T < c_\gamma) \dot{\sim} Q \mid \mathbf{1}(T_\infty < c_\gamma)$. The results (S18) and (S19) follow. □

Proof of Theorem 2.

Proof. Recall that $\widehat{\psi}_{\text{elas}}$ satisfies

$$n^{-1/2} \sum_{i \in \mathcal{A} \cup \mathcal{B}} \{\delta_i S_{\widehat{\psi}_{\text{elas}}}(V_i; \widehat{\eta}_1) + \mathbf{1}(T < c_\gamma)(1 - \delta_i) S_{\widehat{\psi}_{\text{elas}}}(V_i; \widehat{\alpha}, \widehat{\eta}_0)\} = 0.$$

We discuss two cases with $T < c_\gamma$ and $T \geq c_\gamma$ separately.

First, conditional on $T < c_\gamma$, $\widehat{\psi}_{\text{elas}}$ satisfies $0 = n^{-1/2} \sum_{i \in \mathcal{A} \cup \mathcal{B}} \{\delta_i S_{\widehat{\psi}_{\text{elas}}}(V_i; \widehat{\eta}_1) + (1-\delta_i) S_{\widehat{\psi}_{\text{elas}}}(V_i; \widehat{\alpha}, \widehat{\eta}_0)\}$. By the Taylor expansion, we then have

$$\begin{aligned} n^{1/2}(\widehat{\psi}_{\text{elas}} - \psi_0) \mid (T < c_\gamma) &= \left\{ -\mathcal{I}_{\text{eff}}^{-1} n^{-1/2} \sum_{i \in \mathcal{A} \cup \mathcal{B}} S_{\psi_0}(V_i) + o_{\mathbb{P}}(1) \right\} \Bigg| (T < c_\gamma) \\ &\dot{\sim} \mathcal{N}_{\text{eff}} \mid (T_\infty < c_\gamma), \end{aligned} \tag{S20}$$

where $\mathcal{I}_{\text{eff}} = \rho \mathcal{I}_{\text{rt}} + \mathcal{I}_{\text{rw}}$, $o_{\mathbb{P}}(1)$ follows by a similar argument for (S5), and $\dot{\sim}$ follows by Proposition S3.

Second, conditional on $T \geq c_\gamma$, $\widehat{\psi}_{\text{elas}}$ satisfies $n^{-1/2} \sum_{i \in \mathcal{A}} \widehat{S}_{\widehat{\psi}_{\text{elas}}}(V_i) = 0$. By the Taylor expansion, we then have

$$\begin{aligned} n^{1/2}(\widehat{\psi}_{\text{elas}} - \psi_0) \mid (T \geq c_\gamma) &= \left\{ -\mathcal{I}_{\text{rt}}^{-1} \left(\frac{m}{n}\right)^{1/2} m^{-1/2} \sum_{i \in \mathcal{A}} S_{\psi_0}(V_i) + o_{\mathbb{P}}(1) \right\} \Bigg| (T \geq c_\gamma) \\ &\dot{\sim} \mathcal{N}_{\text{rt}} \mid (T_\infty \geq c_\gamma), \end{aligned} \tag{S21}$$

where $o_{\mathbb{P}}(1)$ follows by a similar argument for (S5), and $\dot{\sim}$ follows by Proposition S3. □

S2.3 Characterization of normal distributions with elliptical truncations

We characterize the multivariate normal distributions with elliptical truncations (Tallis, 1963) by MGFs. Let $F_k(\cdot)$ represent the cumulative density function of a chi-square distribution with degrees of freedom k. Let $F_k(\cdot; \lambda)$ represent the cumulative density function of a non-central chi-square distribution with degrees of freedom k and non-centrality parameter λ. Proposition S4 is a general result.

Proposition S4. Let $\mathcal{Z}_1$ follows Normal$(\mu_1, I_{p \times p})$. Then, the MGF of the truncated normal distribution $\mathcal{Z}_1 \mid \mathcal{Z}_1^{\mathrm{T}} \mathcal{Z}_1 \geq a$ is

$$m(t) = \frac{\exp(-\frac{1}{2}\mu_1^{\mathrm{T}}\mu_1) \sum_{k=0}^{\infty} \{1 - F_{p+2k}(a)\} \{(\mu_1 + t)^{\mathrm{T}}(\mu_1 + t)/2\}^k / k!}{1 - F_p(a; \mu_1^{\mathrm{T}}\mu_1)}. \tag{S22}$$

The first and second moments of $\mathcal{Z}_1 \mid \mathcal{Z}_1^{\mathrm{T}} \mathcal{Z}_1 \geq a$ are

$$\mathbb{E}(\mathcal{Z}_1 \mid \mathcal{Z}_1^{\mathrm{T}} \mathcal{Z}_1 \geq a) = \mu_1 \cdot \frac{1 - F_{p+2}(a; \mu_1^{\mathrm{T}}\mu_1)}{1 - F_p(a; \mu_1^{\mathrm{T}}\mu_1)}, \tag{S23}$$

$$\mathbb{E}(\mathcal{Z}_1^{\otimes 2} \mid \mathcal{Z}_1^{\mathrm{T}} \mathcal{Z}_1 \geq a) = I_{p \times p} \frac{1 - F_{p+2}(a; \mu_1^{\mathrm{T}}\mu_1)}{1 - F_p(a; \mu_1^{\mathrm{T}}\mu_1)} + \mu_1 \mu_1^{\mathrm{T}} \frac{1 - F_{p+4}(a; \mu_1^{\mathrm{T}}\mu_1)}{1 - F_p(a; \mu_1^{\mathrm{T}}\mu_1)}. \tag{S24}$$

As a sanity check, we verify that for $a = 0$, $m(t)$ is the MGF of a normal distribution with mean

μ_1 and variance $I_{p\times p}$. When $a = 0$, $F_{p+2k}(a) = 0$ for all $k \geq 0$. Therefore, (S22) reduces to

$$\begin{aligned} m(t) &= \exp(-\frac{1}{2}\mu_1^{\mathrm{T}}\mu_1)\sum_{k=0}^{\infty}\{(\mu_1+t)^{\mathrm{T}}(\mu_1+t)/2\}^k/k! \\ &= \exp(-\frac{1}{2}\mu_1^{\mathrm{T}}\mu_1)\{\exp(\mu_1+t)^{\mathrm{T}}(\mu_1+t)/2\} \\ &= \exp(\mu_1^{\mathrm{T}}t + \frac{1}{2}t^{\mathrm{T}}t), \end{aligned}$$

corresponding to the MGF of Normal$(\mu_1, I_{p\times p})$. Moreover, by (S23) and (S24), the mean and variance of $\mathcal{Z}_1$ are

$$\begin{aligned} \mathbb{E}(\mathcal{Z}_1 \mid \mathcal{Z}_1^{\mathrm{T}}\mathcal{Z}_1 \geq 0) &= \mu_1, \\ \mathbb{E}(\mathcal{Z}_1^2 \mid \mathcal{Z}_1^{\mathrm{T}}\mathcal{Z}_1 \geq 0) &= I_{p\times p} + \mu_1\mu_1^{\mathrm{T}}, \end{aligned}$$

respectively, corresponding to the mean and variance of Normal$(\mu_1, I_{p\times p})$.

Proof. Define a set $\mathbb{C} = \{\mathcal{Z}_1 \in \mathbb{R}^p : \mathcal{Z}_1^{\mathrm{T}}\mathcal{Z}_1 \geq a\}$. We derive the MGF $m(t)$ for $\mathcal{Z}_1$ in the subspace $\mathbb{C}$. By definition, we have

$$\begin{aligned} m(t) &= \mathbb{E}\{\exp(t^{\intercal}Z_1)\} \\ &\propto \int_{\mathbb{C}} \exp(t^{\mathrm{T}}z)\exp\left\{-\frac{1}{2}(z-\mu_1)^{\mathrm{T}}(z-\mu_1)\right\}dz \\ &\propto \exp\left(\frac{1}{2}t^{\mathrm{T}}t + \mu_1^{\mathrm{T}}t\right)\int_{\mathbb{C}} \exp\left\{-\frac{1}{2}(z-\mu_1-t)^{\mathrm{T}}(z-\mu_1-t)\right\}dz. \end{aligned} \tag{S25}$$

Let $\mathcal{Z}^{\mathrm{T}}\mathcal{Z}$ follow a non-central chi-square distribution with parameters p and $(\mu_1+t)^{\mathrm{T}}(\mu_1+t)$. The probability of $\mathcal{Z}^{\mathrm{T}}\mathcal{Z} \geq a$ can be characterized by (Tallis, 1963)

$$\begin{aligned} P(\mathcal{Z}^{\mathrm{T}}\mathcal{Z} \geq a) &= \exp\{-(\mu_1+t)^{\mathrm{T}}(\mu_1+t)/2\}\sum_{k=0}^{\infty}\{1-F_{p+2k}(a)\}\{(\mu_1+t)^{\mathrm{T}}(\mu_1+t)/2\}^k/k! \\ &= (2\pi)^{-p/2}\int_{\mathbb{C}}\exp\left\{-\frac{1}{2}(z-\mu_1-t)^{\mathrm{T}}(z-\mu_1-t)\right\}dz. \end{aligned}$$

Continuing with (S25), we have

$$m(t) \propto \exp(-\frac{1}{2}\mu_1^{\mathrm{T}}\mu_1)\sum_{k=0}^{\infty}\{1-F_{p+2k}(a)\}\{(\mu_1+t)^{\mathrm{T}}(\mu_1+t)/2\}^k/k!.$$

Because $m(0) = 1$, (S22) follows.

Let the normalizing constant be $C = \exp\left(-\frac{1}{2}\mu_1^{\mathrm{T}}\mu_1\right)\sum_{k=0}^{\infty}\{1-F_{p+2k}(a)\}(\mu_1^{\mathrm{T}}\mu_1/2)^k/k! = 1 - F_p(a;\mu_1^{\mathrm{T}}\mu_1)$. Taking the directive of $Cm(t)$ with respect to t and evaluating at $t = 0$, we have $C\,\mathrm{d}m(t)/\mathrm{d}t|_{t=0}$ becomes

$$(\mu_1+t)\exp\left(-\frac{1}{2}\mu_1^{\mathrm{T}}\mu_1\right)\sum_{k=0}^{\infty}\{1-F_{p+2k+2}(a)\}\{(\mu_1+t)^{\mathrm{T}}(\mu_1+t)/2\}^k/k!\Big|_{t=0}$$

$$
\begin{aligned}
&= \mu_1 \exp\left(-\frac{1}{2}\mu_1^{\mathrm{T}}\mu_1\right)\sum_{k=0}^{\infty}\{1-F_{p+2k+2}(a)\}(\mu_1^{\mathrm{T}}\mu_1/2)^k/k! \\
&= \mu_1\left\{1-F_{p+2}(a;\mu_1^{\mathrm{T}}\mu_1)\right\}.
\end{aligned}
$$

Thus, the first moment of $\mathcal{Z}_1 \mid \mathcal{Z}_1^{\mathrm{T}}\mathcal{Z}_1 \geq a$ is

$$
\begin{aligned}
\mathbb{E}(\mathcal{Z}_1 \mid \mathcal{Z}_1^{\mathrm{T}}\mathcal{Z}_1 \geq a) &= \mu_1 \frac{\sum_{k=0}^{\infty}\{1-F_{p+2k+2}(a)\}(\mu_1^{\mathrm{T}}\mu_1/2)^k/k!}{\sum_{k=0}^{\infty}\{1-F_{p+2k}(a)\}(\mu_1^{\mathrm{T}}\mu_1/2)^k/k!}, \\
&= \mu_1 \frac{1-F_{p+2}(a;\mu_1^{\mathrm{T}}\mu_1)}{1-F_{p}(a;\mu_1^{\mathrm{T}}\mu_1)},
\end{aligned}
$$

as in (S23).

Taking the second directive of $Cm(t)$ with respect to t and evaluating at $t = 0$, we have $C\,\mathrm{d}^2m(t)/\mathrm{d}t^2\big|_{t=0}$ becomes

$$
\begin{aligned}
&\exp\left(-\frac{1}{2}\mu_1^{\mathrm{T}}\mu_1\right)\left[\sum_{k=0}^{\infty}\{1-F_{p+2k+2}(a)\}\{(\mu_1+t)^{\mathrm{T}}(\mu_1+t)/2\}^k/k!\Big|_{t=0}\right. \\
&\left.+(\mu_1+t)(\mu_1+t)^{\mathrm{T}}\sum_{k=0}^{\infty}\{1-F_{p+2k+4}(a)\}\{(\mu_1+t)^{\mathrm{T}}(\mu_1+t)/2\}^k/k!\Big|_{t=0}\right] \\
= &\exp\left(-\frac{1}{2}\mu_1^{\mathrm{T}}\mu_1\right)\left[\sum_{k=0}^{\infty}\{1-F_{p+2k+2}(a)\}(\mu_1^{\mathrm{T}}\mu_1/2)^k/k! + \mu_1\mu_1^{\mathrm{T}}\sum_{k=0}^{\infty}\{1-F_{p+2k+4}(a)\}(\mu_1^{\mathrm{T}}\mu_1/2)^k/k!\right] \\
= &\ I_{p\times p}\{1-F_{p+2}(a;\mu_1^{\mathrm{T}}\mu_1)\} + \mu_1\mu_1^{\mathrm{T}}\{1-F_{p+4}(a;\mu_1^{\mathrm{T}}\mu_1)\},
\end{aligned}
$$

Thus, the second moment of $\mathcal{Z}_1 \mid \mathcal{Z}_1^{\mathrm{T}}\mathcal{Z}_1 \geq a$ is

$$
\begin{aligned}
\mathbb{E}(\mathcal{Z}_1^{\otimes 2} \mid \mathcal{Z}_1^{\mathrm{T}}\mathcal{Z}_1 \geq a) &= I_{p\times p}\frac{\sum_{k=0}^{\infty}\{1-F_{p+2k+2}(a)\}(\mu_1^{\mathrm{T}}\mu_1/2)^k/k!}{\sum_{k=0}^{\infty}\{1-F_{p+2k}(a)\}(\mu_1^{\mathrm{T}}\mu_1/2)^k/k!} \\
&\quad +\mu_1\mu_1^{\mathrm{T}}\frac{\sum_{k=0}^{\infty}\{1-F_{p+2k+4}(a)\}(\mu_1^{\mathrm{T}}\mu_1/2)^k/k!}{\sum_{k=0}^{\infty}\{1-F_{p+2k}(a)\}(\mu_1^{\mathrm{T}}\mu_1/2)^k/k!}. \\
&= I_{p\times p}\frac{1-F_{p+2}(a;\mu_1^{\mathrm{T}}\mu_1)}{1-F_{p}(a;\mu_1^{\mathrm{T}}\mu_1)} + \mu_1\mu_1^{\mathrm{T}}\frac{1-F_{p+4}(a;\mu_1^{\mathrm{T}}\mu_1)}{1-F_{p}(a;\mu_1^{\mathrm{T}}\mu_1)}.
\end{aligned}
$$

as in (S24). □

Proof of the decomposition $\mathcal{N}_{\mathrm{rt}} = V_{\text{rt-eff}}^{1/2}\mathcal{Z}_1 - V_{\mathrm{eff}}^{1/2}\mathcal{Z}_2$.

Proof. First, we show

$$
\begin{aligned}
(\mathcal{I}_{\mathrm{rw}}+\rho\mathcal{I}_{\mathrm{rt}})^{-1}(\rho^{1/2}+\Gamma^{\mathrm{T}}) &= (\mathcal{I}_{\mathrm{rw}}+\rho\mathcal{I}_{\mathrm{rt}})^{-1}(\rho^{1/2}+\mathcal{I}_{\mathrm{rt}}^{-1}\mathcal{I}_{\mathrm{rw}}\rho^{-1/2}) \\
&= (\mathcal{I}_{\mathrm{rw}}+\rho\mathcal{I}_{\mathrm{rt}})^{-1}(\rho\mathcal{I}_{\mathrm{rt}}+\mathcal{I}_{\mathrm{rw}})\mathcal{I}_{\mathrm{rt}}^{-1}\rho^{-1/2} \\
&= (\rho\mathcal{I}_{\mathrm{rt}})^{-1}\rho^{1/2}.
\end{aligned}
$$

Then, we have

$$
\mathcal{N}_{\mathrm{rt}}(\mathcal{Z}_{\mathrm{rt}}) = -(\rho\mathcal{I}_{\mathrm{rt}})^{-1}(\rho^{1/2}\mathcal{Z}_{\mathrm{rt}})
$$

$$
\begin{aligned}
&= -(\mathcal{I}_{\mathrm{rw}} + \rho\mathcal{I}_{\mathrm{rt}})^{-1}(\rho^{1/2} + \Gamma^{\mathrm{T}})\mathcal{Z}_{\mathrm{rt}} \\
&= -(\rho\mathcal{I}_{\mathrm{rt}} + \mathcal{I}_{\mathrm{rw}})^{-1}(\mathcal{Z}_{\mathrm{rw}} + \rho^{1/2}\mathcal{Z}_{\mathrm{rt}}) + (\rho\mathcal{I}_{\mathrm{rt}} + \mathcal{I}_{\mathrm{rw}})^{-1}(\mathcal{Z}_{\mathrm{rw}} - \Gamma^{\mathrm{T}}\mathcal{Z}_{\mathrm{rt}}) \\
&= -(\rho\mathcal{I}_{\mathrm{rt}} + \mathcal{I}_{\mathrm{rw}})^{-1/2}\left\{V_{\mathrm{eff}}^{1/2}(\mathcal{Z}_{\mathrm{rw}} + \rho^{1/2}\mathcal{Z}_{\mathrm{rt}})\right\} + \left\{(\rho\mathcal{I}_{\mathrm{rt}} + \mathcal{I}_{\mathrm{rw}})^{-1}\Sigma_{SS}^{1/2}\right\}\left\{\Sigma_{SS}^{-1/2}(\mathcal{Z}_{\mathrm{rw}} - \Gamma^{\mathrm{T}}\mathcal{Z}_{\mathrm{rt}})\right\} \\
&= -(\rho\mathcal{I}_{\mathrm{rt}} + \mathcal{I}_{\mathrm{rw}})^{-1/2}\mathcal{Z}_2 + \left\{(\rho\mathcal{I}_{\mathrm{rt}} + \mathcal{I}_{\mathrm{rw}})^{-1}\Sigma_{SS}^{1/2}\right\}\mathcal{Z}_1 \\
&= -(\rho\mathcal{I}_{\mathrm{rt}} + \mathcal{I}_{\mathrm{rw}})^{-1/2}\mathcal{Z}_2 + \left\{(\rho\mathcal{I}_{\mathrm{rt}})^{-1} - (\rho\mathcal{I}_{\mathrm{rt}} + \mathcal{I}_{\mathrm{rw}})^{-1}\right\}^{1/2}\mathcal{Z}_1 \\
&= -V_{\mathrm{eff}}^{1/2}\mathcal{Z}_2 + V_{\text{rt-eff}}^{1/2}\mathcal{Z}_1.
\end{aligned}
$$

□

S3 Technical details for inference

S3.1 Inconsistency of the nonparametric bootstrap

Theorem S1. Let $\widehat{\psi}^*_{\mathrm{elas}}$ be the nonparametric bootstrap replicate of $\widehat{\psi}_{\mathrm{elas}}$. Under assumptions in Theorem 1, the bootstrap distribution of $n^{1/2}(\widehat{\psi}^*_{\mathrm{elas}} - \widehat{\psi}_{\mathrm{elas}})$ give the observed data is inconsistent for the distribution of $n^{1/2}(\widehat{\psi}_{\mathrm{elas}} - \psi_0)$.

The reason for the inconsistency of the bootstrap estimator is exactly that $\mathbf{1}(T < c_\gamma) = 0$ does not imply that Assumption 2 is violated. When this happens, $\mathbf{1}(T^* < c_\gamma)$ is asymptotically non-degenerate, making the bootstrap estimator inconsistent.

Proof of Theorem S1.

Proof. We now show that the nonparametric bootstrap inference for $\widehat{\psi}_{\mathrm{elas}}$ is inconsistent.

Let the bootstrap RT and RW resamples be indexed by $\mathcal{A}^*$ and $\mathcal{B}^*$, respectively. Denote the bootstrap replicates of $\widehat{\psi}_{\mathrm{rt}}$, $\widehat{\alpha}$, and $\widehat{\eta}^{\mathrm{T}} = (\widehat{\eta}_0^{\mathrm{T}}, \widehat{\eta}_1^{\mathrm{T}})$ as $\widehat{\psi}^*_{\mathrm{rt}}$, $\widehat{\alpha}^*$, and $\widehat{\eta}^{*\mathrm{T}} = (\widehat{\eta}_0^{*\mathrm{T}}, \widehat{\eta}_1^{*\mathrm{T}})$, respectively. Then the bootstrap replicate of T is

$$
T^* = \left\{\sum_{i\in\mathcal{B}^*} S_{\mathrm{rw},\widehat{\psi}^*_{\mathrm{rt}}}(V_i; \widehat{\alpha}^*, \widehat{\eta}_0^*)\right\}^{\mathrm{T}} \widehat{\Sigma}_{SS}^{*-1}\left\{\sum_{i\in\mathcal{B}^*} S_{\mathrm{rw},\widehat{\psi}^*_{\mathrm{rt}}}(V_i; \widehat{\alpha}^*, \widehat{\eta}_0^*)\right\}. \tag{S26}
$$

The bootstrap replicate $\widehat{\psi}^*_{\mathrm{elas}}$ solves

$$
\sum_{i\in\mathcal{A}^*\cup\mathcal{B}^*}\{\delta_i S_\psi(V_i; \widehat{\eta}_1^*) + \mathbf{1}(T^* < c_\gamma)(1-\delta_i)S_\psi(V_i; \widehat{\alpha}^*, \widehat{\eta}_0^*)\} = 0. \tag{S27}
$$

By the Taylor expansion, we have

$$
\begin{aligned}
& n^{1/2}(\widehat{\psi}^*_{\mathrm{elas}} - \widehat{\psi}_{\mathrm{elas}}) \\
&= -(\Gamma^{\mathrm{T}}_{\mathrm{elas}})^{-1}n^{-1/2}\sum_{i\in\mathcal{A}^*\cup\mathcal{B}^*}\left\{\delta_i S_{\widehat{\psi}_{\mathrm{elas}}}(V_i) + \mathbf{1}(T^* < c_\gamma)(1-\delta_i)S_{\widehat{\psi}_{\mathrm{elas}}}(V_i)\right\} + o_{\mathbb{P}}(1) \qquad \text{(S28)} \\
&= -(\Gamma^{\mathrm{T}}_{\mathrm{elas}})^{-1}n^{-1/2}\sum_{i\in\mathcal{A}^*\cup\mathcal{B}^*}\{\delta_i S_{\psi_0}(V_i) + \mathbf{1}(T^* < c_\gamma)(1-\delta_i)S_{\psi_0}(V_i)\} \\
& \quad -(\Gamma^{\mathrm{T}}_{\mathrm{elas}})^{-1}n^{-1}\sum_{i\in\mathcal{A}^*\cup\mathcal{B}^*}\left\{\delta_i\frac{\partial S_{\psi_0}(V_i)}{\partial\psi^{\mathrm{T}}} + \mathbf{1}(T^* < c_\gamma)(1-\delta_i)\frac{\partial S_{\psi_0}(V_i)}{\partial\psi^{\mathrm{T}}}\right\}
\end{aligned}
$$

$$\times n^{1/2}(\widehat{\psi}_{\text{elas}} - \psi_0) + o_{\mathbb{P}}(1). \tag{S29}$$

Suppose that the observed T is $T \geq c_\gamma$. Then by (S20),

$$\begin{aligned} n^{1/2}(\widehat{\psi}_{\text{elas}} - \psi_0) &= -(\Gamma_{\text{elas}}^{\text{T}})^{-1} n^{-1/2} \sum_{i \in \mathcal{A} \cup \mathcal{B}} \delta_i S_{\psi_0}(V_i) + o_{\mathbb{P}}(1) \\ &\dot{\sim} -(\Gamma_{\text{elas}}^{\text{T}} \rho^{1/2})^{-1} \mathcal{Z}_{\text{rt}}. \end{aligned}$$

Let $\mathcal{Z}_{\text{rt}}^* \sim \mathcal{N}(\mathcal{Z}_{\text{rt}}, \mathcal{I}_{\text{rt}})$ and $\mathcal{Z}_{\text{rw}}^* \sim \mathcal{N}(\mathcal{Z}_{\text{rw}}, \mathcal{I}_{\text{rw}})$. Then, (S29) becomes

$$\begin{aligned} &\dot{\sim} -(\Gamma_{\text{elas}}^{\text{T}} \rho^{1/2})^{-1} \left\{ \mathcal{Z}_{\text{rt}}^* + \mathbf{1}(T^* < c_\gamma) \rho^{1/2} \mathcal{Z}_{\text{rw}}^* \right\} + (\Gamma_{\text{elas}}^{\text{T}} \rho^{1/2})^{-1} \mathcal{Z}_{\text{rt}} \\ &= -(\Gamma_{\text{elas}}^{\text{T}} \rho^{1/2})^{-1} \left\{ \mathcal{Z}_{\text{rt}}^* - \mathcal{Z}_{\text{rt}} + \mathbf{1}(T^* < c_\gamma) \rho^{1/2} \mathcal{Z}_{\text{rw}}^* \right\} \\ &= -(\Gamma_{\text{elas}}^{\text{T}} \rho^{1/2})^{-1} \left\{ \mathcal{Z}_{\text{rt}}^* - \mathcal{Z}_{\text{rt}} + \mathbf{1}(T^* < c_\gamma) \rho^{1/2} (\mathcal{Z}_{\text{rw}}^* - \mathcal{Z}_{\text{rw}}) \right\} \qquad \text{(S30)} \\ &\quad -(\Gamma_{\text{elas}}^{\text{T}} \rho^{1/2})^{-1} \mathbf{1}(T^* < c_\gamma) \rho^{1/2} \mathcal{Z}_{\text{rw}} \qquad \text{(S31)} \end{aligned}$$

Note, (S30) has the same limiting distribution as $n^{1/2}(\widehat{\psi}_{\text{elas}} - \psi_0)$, while (S31) is asymptotically non-degenerate. Therefore, the bootstrap inference is inconsistent. □

S3.2 Proof of Theorem 3

Proof. Under the local alternatives, we have

$$\begin{aligned} &\lim_{n \to \infty} \mathbb{P} \left\{ n^{1/2} e_k^{\text{T}} (\widehat{\psi}_{\text{elas}} - \psi_0) \in \text{ECI}_{k,1-\alpha} \right\} \\ \geq\ &\lim_{n \to \infty} \mathbb{P} \left\{ n^{1/2} e_k^{\text{T}} (\widehat{\psi}_{\text{elas}} - \psi_0) \in [\inf_{\mu_1 \in \mathcal{B}_{1-\widetilde{\alpha}}} \widehat{Q}_{k,\widetilde{\alpha}/2}(\mu_1), \sup_{\mu_1 \in \mathcal{B}_{1-\widetilde{\alpha}}} \widehat{Q}_{k,1-\widetilde{\alpha}/2}(\mu_1)] \mid \mu_1 \in \mathcal{B}_{1-\widetilde{\alpha}} \right\} \times (1 - \widetilde{\alpha}) \\ \geq\ &(1 - \widetilde{\alpha})^2 = 1 - \alpha. \end{aligned}$$

Under the fixed alternative, we have

$$\begin{aligned} &\lim_{n \to \infty} \mathbb{P} \left\{ n^{1/2} e_k^{\text{T}} (\widehat{\psi}_{\text{elas}} - \psi_0) \in \text{ECI}_{k,1-\alpha} \right\} \\ =\ &\lim_{n \to \infty} \mathbb{P} \left\{ n^{1/2} e_k^{\text{T}} (\widehat{\psi}_{\text{elas}} - \psi_0) \in [\widehat{Q}_{k,\alpha/2}(\pm\infty), \widehat{Q}_{k,1-\alpha/2}(\pm\infty)] \right\} = 1 - \alpha. \end{aligned}$$

□

S4 Additional simulation results and studies

S4.1 Comparing AIPW and SES

In this simulation study, we compare the performances of the AIPW-adjusted approach and the SES approach based on RT data. The data generating mechanism is the same as in Section 4 except that we now consider different propensity score distributions. Specifically, consider $A \mid X, \delta = 1 \sim$ Bernoulli$\{e_1(X)\}$, where logit $e_1(X) = \alpha_0 + \alpha_1 X_1 + \alpha_2 X_2$ and

i) (weak separation of propensity score distributions by treatment group) $\alpha = (-2, -1, -1)$,

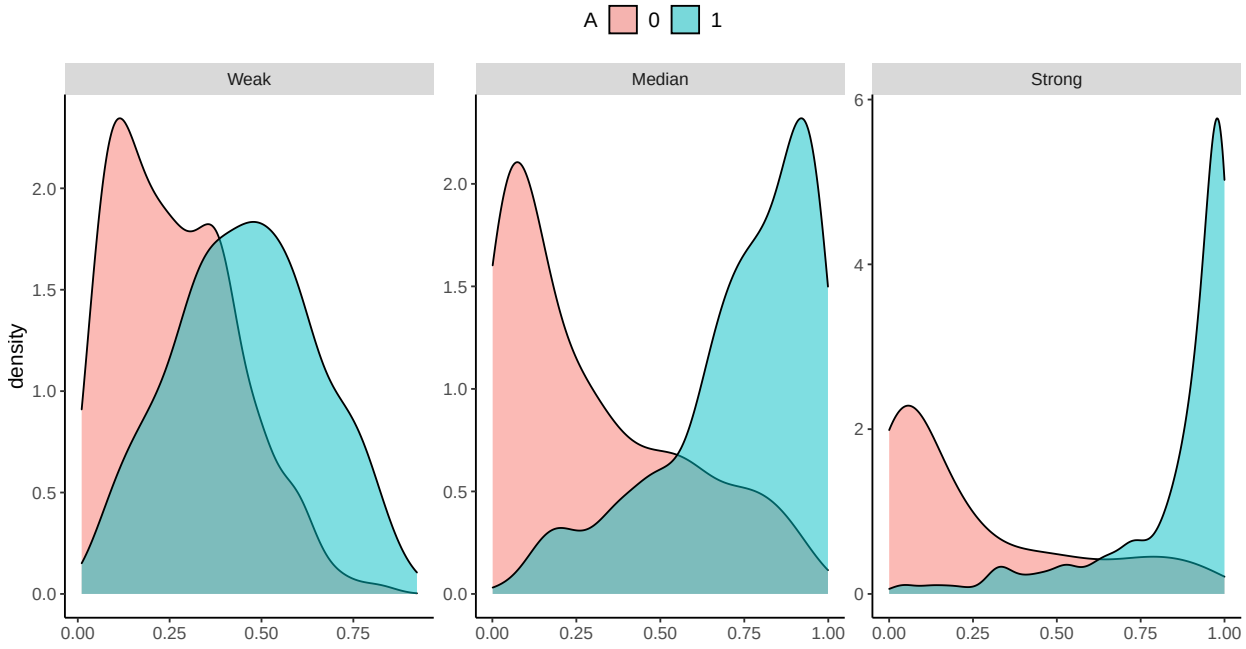


Figure S1: Illustration of the propensity score distributions by treatment group under weak, median and strong separations (Section S4.1).

ii) (median separation of propensity score distributions by treatment group) $\alpha = (-2, -2, -2)$,

iii) (strong separation of propensity score distributions by treatment group) $\alpha = (-2, -3, -3)$.

Figure S1 shows the propensity score distributions by treatment group and demonstrates the degrees of separation in the three scenarios.

The estimators for comparison are the following:

a) RT.AIPW: the AIPW-adjustment outcome approach of Kennedy (2020) that fits

$$\frac{A_i\{Y_i - \widehat{\mu}_{\delta,1}(X_i)\}}{\widehat{e}_\delta(X_i)} - \frac{(1-A_i)\{Y_i - \widehat{\mu}_\delta(X_i)\}}{1-\widehat{e}_\delta(X_i)} + \widehat{\mu}_{\delta,1}(X_i) - \widehat{\mu}_\delta(X_i)$$

against Z_i based only on the RT data, where $\mu_{\delta,1}(X_i) = \mathbb{E}\{Y(1) \mid X, \delta = 1\}$, and

b) RT.SES: the efficient estimator based only on the RT data solving the SES (9) with the combining indicator $\mathbf{1}(T < c_\gamma) \equiv 0$.

Table S2 reports the simulation results for comparing RT.AIPW and RT.SES. Across the three cases, both estimators have small biases. RT.AIPW has larger variances and MSEs than RT.SES. By construction, RT.AIPW takes the inverse of the estimated propensity scores the to remove confounding biases, which can be unstable when some propensity scores are close to zero or one. Differently, the SES in (6) uses the mean independence of $H_{\psi_0} - \mu_\delta(X)$ and $A - e_\delta(X)$ to construct unbiased estimating equations, thus avoiding taking the inverse of the estimated propensity score.

Table S2: Simulation results of Monte Carlo biases, standard deviations and root-mean-square errors of estimators in the three cases: weak separation $\alpha = (-2, -1, -1)$, median separation $\alpha = (-2, -2, -2)$, and strong separation $\alpha = (-2, -3, -3)$ with $n = 2000$ regarding the performances of the AIPW-adjusted outcome approach (labeled as RT.AIPW) and the SES approach (labeled as RT.SES) (Section S4.1)

	RT.AIPW		RT.SES		RT.AIPW		RT.SES		RT.AIPW		RT.SES	
	Case 1: weak separation				Case 2: median separation				Case 3: strong separation			
	$\psi_1 = 1$	$\psi_2 = 1$	$\psi_1 = 1$	$\psi_2 = 1$	$\psi_1 = 1$	$\psi_2 = 1$	$\psi_1 = 1$	$\psi_2 = 1$	$\psi_1 = 1$	$\psi_2 = 1$	$\psi_1 = 1$	$\psi_2 = 1$
Bias ($\times 10^{-2}$)	-1	-2	-1	-1	1	-1	0	-1	3	1	-2	-2
S.D. ($\times 10^{-3}$)	242	248	180	186	365	381	260	249	622	555	394	397
root-MSE ($\times 10^{-3}$)	242	249	180	186	365	381	260	250	623	555	394	397
Coverage rate (%)	94.4	91.8	95.4	93.2	92.8	93.2	94.6	94.6	91.0	92.0	93.2	91.6
Width ($\times 10^{-3}$)	955	942	709	710	1390	1420	974	971	14569	5077	1448	1448

S4.2 Additional simulation results in Section 4

Table S3 reports the detailed numerical results of the estimators in Section 4, including absolute biases, standard deviations, and MSEs. In addition, Tables S4 and S6 report the numerical results of the estimators, including absolute biases, standard deviations, and MSEs, and the confidence intervals, including coverage rates and widths when $m = 5000$. Table S8 reports Monte Carlo averages and standard deviations of the estimators for the local parameter η, the threshold c_γ, and the proportion of combining the RT and RW samples.

S4.3 Importance of overlapping between the RT and RW samples

This simulation study creates an artificial scenario to illustrate the danger of extrapolation when transporting from the narrow RT sample to the broader RW sample with the HTE transportability and overlap assumption violated. Instead of the data generation distributions in Section 4, we consider a new data distribution, in which $X_1, X_2 \sim \mathcal{N}(0, 1)$ for both RT and RW finite population. For the HTE, we now consider $\tau(Z) = \psi_0 + \psi_1 X_1 + \psi_2 |X_2|$ with $\psi_0 = 0, \psi_1 = \psi_2 = 1$. To generate the RT sample, we first generate the RT selection indicator by $\delta \mid X \sim \text{Bernoulli}\{\pi_\delta(X)\}$, where $\text{logit}\{\pi_\delta(X)\} = -4.5 - 2X_1 - 2X_2$, and then set $\delta = 0$ if $X_2 < 0$. We also select a random sample of size $m = 2000$ from the population to form an RW sample. In this case, the RT sample is a narrower sample where X_2 can only be positive. The HTE for the RT sample (and the overlap RW sample) is $\tau(Z) = \psi_0 + \psi_1 X_1 + \psi_2 X_2$, but the HTE for the non-overlap region of the RW sample is not. In the RW sample, we consider $b = 0$ to represent a scenario without unmeasured confounding for treatment assignment.

Table S9 reports the simulation results. The RT estimator $\widehat{\psi}_{\text{rt}}$ has small biases. Even without unmeasured confounding, the efficient combining estimator $\widehat{\psi}_{\text{eff}}$ is biased with low coverage rates for all parameters, due to model misspecification of the HTE for the RW population and violation of Assumption 2(i) and (iii). The elastic combining approach rejects the RW sample for combining by 97% times over simulation, and thus $\widehat{\psi}_{\text{elas}}$ stays close to $\widehat{\psi}_{\text{rt}}$ and has small biases and satisfactory coverage properties.

S4.4 Sensitivity analysis of ECIs to the choice of the cut-off value κ_n

In this simulation study, we conduct a sensitivity analysis to assess the performance of the ECIs to the choice of the cut-off value κ_n. All data generating distributions are the same as in Section 4. Table S10 reports the sensitivity results of coverage rates and widths of the ECIs to the choice of the cut-off value $\kappa_n \in \{0.5(\log n)^{1/2}, (\log n)^{1/2}\}$. When b is small, the width of the ECIs decreases with κ_n, while when b is large, the coverage rate and width of the ECIs increase with κ_n. To help explain the results, denote $\text{ECI}^{[1]}_{k,1-\alpha} = [\inf_{\eta\in\mathcal{B}_{1-\widetilde{\alpha}}} \widehat{Q}_{k,\widetilde{\alpha}/2}(\mu_1), \sup_{\eta\in\mathcal{B}_{1-\widetilde{\alpha}}} \widehat{Q}_{k,1-\widetilde{\alpha}/2}(\mu_1)]$, $\text{ECI}^{[2]}_{k,1-\alpha} = [\widehat{Q}_{k,\alpha/2}(\pm\infty), \widehat{Q}_{k,1-\alpha/2}(\pm\infty)]$, and $\text{ECI}_{k,1-\alpha} = \text{ECI}^{[1]}_{k,1-\alpha}\mathbf{1}(T \le \kappa_n) + \text{ECI}^{[2]}_{k,1-\alpha}\mathbf{1}(T > \kappa_n)$. When κ_n increases from $0.5(\log n)^{1/2}$ to $(\log n)^{1/2}$, the frequency of choosing $\text{ECI}^{[2]}_{k,1-\alpha}$ over $\text{ECI}^{[1]}_{k,1-\alpha}$ decreases; see $\mathbb{P}(T > \kappa_n)$ reported in Table S11. When b is small, $\text{ECI}^{[2]}_{k,1-\alpha}$ can be more conservative than $\text{ECI}^{[1]}_{k,1-\alpha}$, and when b is large, $\text{ECI}^{[1]}_{k,1-\alpha}$ can be more conservative than $\text{ECI}^{[2]}_{k,1-\alpha}$. This is because when b is small, η is small, the likelihood of integrating the RW sample is large, and $[\widehat{Q}_{k,\widetilde{\alpha}/2}(\mu_1), \widehat{Q}_{k,1-\widetilde{\alpha}/2}(\mu_1)]$ for each small η (thus small μ_1) is narrower than $\text{ECI}^{[2]}_{k,1-\alpha}$, and thus $\text{ECI}^{[2]}_{k,1-\alpha}$ can be more conservative than $\text{ECI}^{[1]}_{k,1-\alpha}$, and vice versa. Overall, the coverage rates and widths of ECIs are close over the choice of κ_n.

S4.5 The elastic combining estimator with a fixed threshold c_γ

In this simulation study, we assess the performance of the elastic combining estimator with a fixed threshold c_γ. All data generating distributions are the same as in Section 4. For the elastic combining estimator, we fix c_γ to be the 95th quantile of a χ^2_3 distribution (i.e., 7.81). Figure 3 presents the plots of Monte Carlo biases, variances, and MSEs of estimators based on 2000 simulated datasets. The elastic integrative estimator $\widehat{\psi}_{\text{elas}}$ with a fixed threshold can increase biases compared to using a data-adaptive selected threshold.

S4.6 Regular inference fails for the pre-test estimator with sample splitting

In this simulation study, we illustrate the failure of regular inference for the pre-test estimator in the context of data integration with sampling splitting. The data generating distribution is the same as in Section 4 except that we double the sample sizes for the RT and RW samples. The RT sample is randomly split into two folds, and similarly, the RW sample is randomly split into two folds. We couple one fold from the RT sample and one fold from the RW sample to form a pre-testing dataset and the rest to form an estimation dataset. In the pre-testing dataset, we conduct the pre-test to decide whether to combine the RT sample and the RW sample. In the estimation dataset, we conduct the analysis based on the decision from the pre-testing, including the point and variance estimation and regular Wald inference. For comparison, we also compute the RT and Eff estimator and their regular Wald inferences.

Table S12 reports the results for the 95% confidence intervals. Similar conclusions in Section 4 can be drawn for the point estimators in this simulation study (not shown). The coverage rates for the RT estimator are close to the nominal level; while the coverage rates for the Eff estimator are more off as b increases. Importantly, the pre-test estimator has poor coverage rates, especially when b is around 0.57, demonstrating the failure of regular inference for the pre-test estimator with

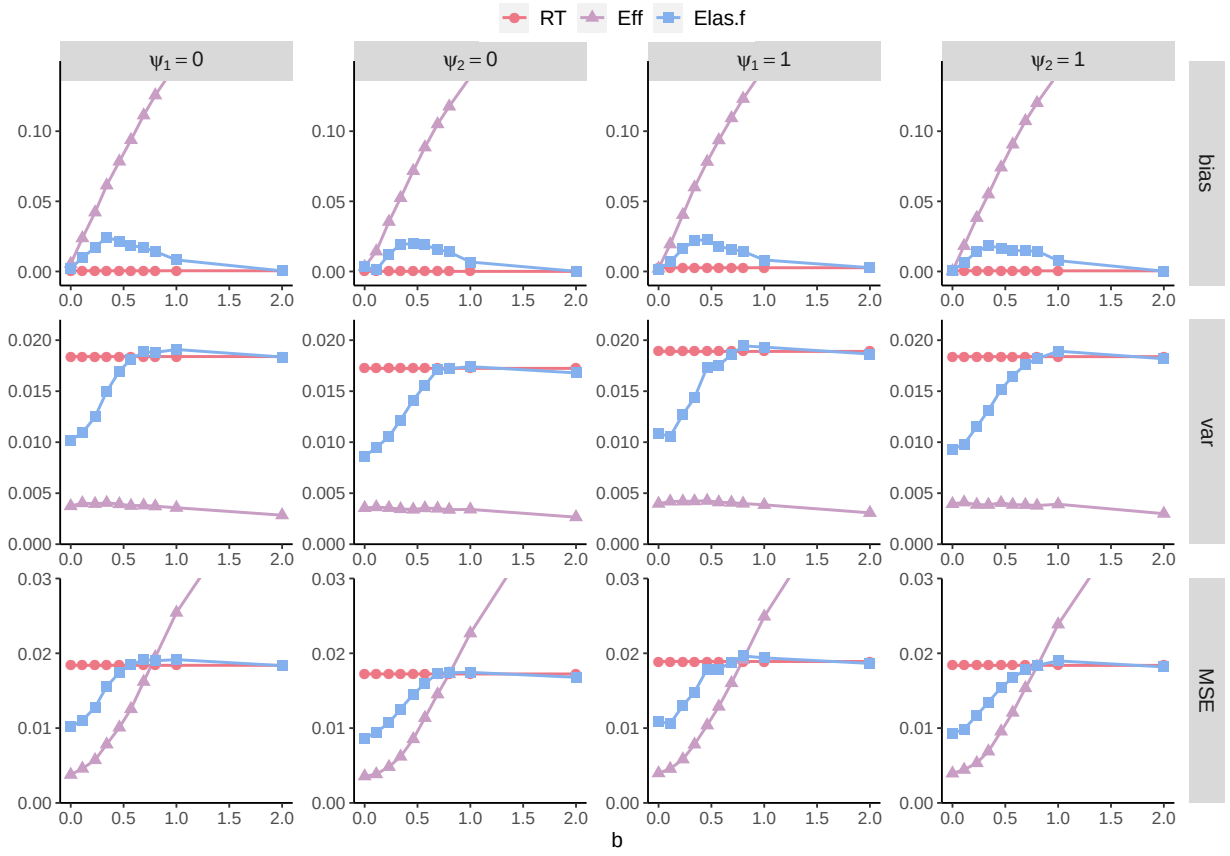


Figure S2: Summary statistics plots of estimators of (ψ_1, ψ_2) with respect to the strength of unmeasured confounding labeled by "b". In each plot, the three estimators are labeled by "RT", "Eff", and "Elas.f" with $c_\gamma \equiv 7.81$ (i.e., the 95th quantile of a χ^2_3 distribution). Each row of the plots corresponds to a different metrics: "bias" for bias, "var" for variance, "MSE" for mean square error; each column of the plots corresponds to one component of (ψ_1, ψ_2) in the two cases: $\psi_1 = 0, \psi_2 = 0$, $\psi_1 = 1$, and $\psi_2 = 1$ with $n = 2000$ (Section S4.5).

sample splitting.

S5 Details of the real-data application

S5.1 Eligibility criteria

The CALGB 9633 trial was designed to determine the efficacy of adjuvant chemotherapy compared with observation with the following eligibility criteria (Strauss et al., 2008):

- Histologically documented non-small cell lung cancer (NSCLC)
- Complete surgical resection (lobectomy or pneumonectomy)
- Stage IB disease (T2N0M0) with tumor size $\geq$ 3cm
- Randomization occurs within 4-8 weeks of surgery
- No prior chemotherapy and radiotherapy for NSCLC

- Age ≥ 18
- Performance status $0 - 1$
- No concomitant malignancy

The NCDB is a clinical oncology registry database that captures the information from approximately 75% of all newly diagnosed cancer patients in the US. Thus, the NCDB involves a more diverse patient population than the RT sample. To make the two RT and RW samples represent the patients from comparable populations, we have used the same eligibility criteria as those of the RT sample to identify eligible patients from the NCDB.

S5.2 Strategies for selecting an RW sample with sufficient overlap with the RT sample

We can employ the following strategies to select an RW sample with sufficient overlap with the RT sample. First, consider the RW sample to be extracted from a large population-based database or electronic health records or claim data. The RT tends to use restrictive criteria in the phase of new treatment evaluation to ensure a more homogeneous patient sample with less severe baseline functional status or comorbidity for safety consideration when testing a new treatment. The large population-based database allows the investigators to find comparable populations or samples by applying the same eligibility criteria of the RT sample to identify comparable RW patients. Second, suppose comparability still fails to achieve by applying the same eligibility criteria. In this case, one can apply an additional matching procedure to improve the comparability between the RT and RW samples and the chance of successfully integrating the information from two separate sources. In our motivating application, we may subsample the cohort of NCDB patients who met the RT eligible criteria. The distribution of baseline covariates, e.g., race, sex, age, histology, and tumor size, can be further matched. Toward this end, one can use various matching algorithms, such as K-nearest neighbor matching, based on the based covariates.

Table S3: Simulation results of Monte Carlo biases, standard deviations, and root-mean-square errors of estimators $\widehat{\psi}_{\text{rt}}$, $\widehat{\psi}_{\text{eff}}$, and $\widehat{\psi}_{\text{elas}}$ (labeled as "RT", "Eff", and "Elastic") in the two cases: zero effect modification $\psi_1 = \psi_2 = 0$ (left) and nonzero effect modification $\psi_1 = \psi_2 = 1$ (right) with $n = 2000$ (Section 4)

	RT		Eff		Elastic		RT		Eff		Elastic	
	Case 1: zero effect modification						Case 2: nonzero effect modification					
b	$\psi_1 = 0$	$\psi_2 = 0$	$\psi_1 = 0$	$\psi_2 = 0$	$\psi_1 = 0$	$\psi_2 = 0$	$\psi_1 = 1$	$\psi_2 = 1$	$\psi_1 = 1$	$\psi_2 = 1$	$\psi_1 = 1$	$\psi_2 = 1$
Bias ($\times 10^{-2}$)												
0	0	0	0	0	0	0	0	0	0	0	0	0
0.11	0	0	-2	-2	0	0	0	0	-2	-2	0	0
0.23	0	0	-4	-4	0	0	0	0	-4	-4	0	0
0.34	0	0	-6	-6	0	1	0	0	-6	-6	0	0
0.46	0	0	-8	-8	1	1	0	0	-8	-8	0	0
0.57	0	0	-9	-9	1	1	0	0	-9	-9	0	0
0.69	0	0	-11	-11	1	1	0	0	-11	-11	0	0
0.8	0	0	-12	-12	1	0	0	0	-12	-12	0	0
1	0	0	-14	-14	0	0	0	0	-14	-15	0	0
2	0	0	-21	-21	0	0	0	0	-21	-21	0	0
S.D. ($\times 10^{-3}$)												
0	136	137	64	63	113	112	135	138	61	63	110	111
0.11	136	137	64	63	114	114	135	138	61	63	111	113
0.23	136	137	65	62	117	116	135	138	61	63	113	115
0.34	136	137	64	62	120	119	135	138	61	62	117	118
0.46	136	137	63	62	122	121	135	138	61	61	121	122
0.57	136	137	62	61	124	125	135	138	59	60	123	126
0.69	136	137	62	60	127	128	135	138	59	60	127	130
0.8	136	137	61	60	128	131	135	138	59	59	128	131
1	136	137	60	60	131	133	135	138	58	58	130	134
2	136	137	53	53	135	136	135	138	52	52	133	137
root-MSE ($\times 10^{-3}$)												
0	136	137	64	63	113	112	135	138	61	63	110	111
0.11	136	137	67	66	115	114	135	138	64	66	111	113
0.23	136	137	76	73	117	116	135	138	72	75	113	115
0.34	136	137	86	84	120	119	135	138	83	85	118	118
0.46	136	137	100	97	122	121	135	138	97	98	121	122
0.57	136	137	112	110	124	125	135	138	109	110	124	126
0.69	136	137	125	124	127	128	135	138	124	124	127	130
0.8	136	137	136	136	128	131	135	138	135	137	128	131
1	136	137	155	156	131	133	135	138	155	156	130	134
2	136	137	214	212	135	136	135	138	212	213	133	137

Table S4: Simulation results of Monte Carlo biases, standard deviations and root-mean-square errors of estimators $\widehat{\psi}_{\text{rt}}$, $\widehat{\psi}_{\text{eff}}$, and $\widehat{\psi}_{\text{elas}}$ (labeled as "RT", "Eff", and "Elastic") in the two cases: zero effect modification $\psi_1 = \psi_2 = 0$ (left) and nonzero effect modification $\psi_1 = \psi_2 = 1$ (right) with $n = 5000$ (Section 4)

	RT		Eff		Elastic		RT		Eff		Elastic	
	Case 1: zero effect modification						Case 2: nonzero effect modification					
b	$\psi_1 = 0$	$\psi_2 = 0$	$\psi_1 = 0$	$\psi_2 = 0$	$\psi_1 = 0$	$\psi_2 = 0$	$\psi_1 = 1$	$\psi_2 = 1$	$\psi_1 = 1$	$\psi_2 = 1$	$\psi_1 = 1$	$\psi_2 = 1$
Bias ($\times 10^{-2}$)												
0	0	0	0	0	0	0	0	0	0	0	0	0
0.11	0	0	-2	-1	1	1	0	0	-1	-1	1	0
0.23	0	0	-3	-3	1	1	0	0	-3	-3	1	1
0.34	0	0	-4	-4	1	1	0	0	-4	-4	1	1
0.46	0	0	-6	-6	1	1	0	0	-6	-6	1	1
0.57	0	0	-7	-7	1	1	0	0	-7	-7	1	1
0.69	0	0	-8	-8	1	1	0	0	-8	-8	0	0
0.8	0	0	-9	-9	0	0	0	0	-9	-9	0	0
1	0	0	-10	-10	0	0	0	0	-10	-10	0	0
2	0	0	-15	-14	0	0	0	0	-14	-15	0	0
S.D. ($\times 10^{-3}$)												
0	136	137	47	45	104	104	135	138	46	45	104	104
0.11	136	137	47	45	105	106	135	138	46	46	103	106
0.23	136	137	47	45	108	110	135	138	45	46	106	108
0.34	136	137	47	44	113	113	135	138	45	46	111	113
0.46	136	137	46	44	118	118	135	138	44	45	117	120
0.57	136	137	46	44	123	123	135	138	44	45	122	125
0.69	136	137	45	44	128	128	135	138	43	44	127	129
0.8	136	137	45	44	131	132	135	138	43	44	130	132
1	136	137	43	43	134	135	135	138	42	42	132	135
2	136	137	37	38	135	136	135	138	37	38	133	137
root-MSE ($\times 10^{-3}$)												
0	136	137	47	45	104	104	135	138	46	45	104	104
0.11	136	137	49	48	106	106	135	138	48	48	103	106
0.23	136	137	55	54	109	110	135	138	54	54	106	109
0.34	136	137	63	62	114	114	135	138	61	63	111	113
0.46	136	137	72	72	119	119	135	138	71	72	117	121
0.57	136	137	81	82	123	124	135	138	80	81	122	125
0.69	136	137	90	91	128	129	135	138	90	91	127	129
0.8	136	137	98	100	131	132	135	138	98	99	130	132
1	136	137	112	113	134	135	135	138	111	113	132	135
2	136	137	150	150	135	136	135	138	149	151	133	137

Table S6: Simulation results of coverage rates and widths of confidence intervals for $\widehat{\psi}_{\text{rt}}$, $\widehat{\psi}_{\text{eff}}$, and $\widehat{\psi}_{\text{elas}}$ (labeled as "RT", "Eff", and "Elastic") in the two cases: zero effect modification $\psi_1 = \psi_2 = 0$ (left) and nonzero effect modification $\psi_1 = \psi_2 = 1$ (right) with $n = 5000$ (Section 4)

	RT		Eff		Elastic		RT		Eff		Elastic	
	Case 1: zero effect modification						Case 2: nonzero effect modification					
b	$\psi_1 = 0$	$\psi_2 = 0$	$\psi_1 = 0$	$\psi_2 = 0$	$\psi_1 = 0$	$\psi_2 = 0$	$\psi_1 = 1$	$\psi_2 = 1$	$\psi_1 = 1$	$\psi_2 = 1$	$\psi_1 = 1$	$\psi_2 = 1$
	Coverage Rate (%)											
0	94.3	94.2	94.4	95.8	94.1	93.0	94.5	93.5	95.3	95.9	94.2	93.2
0.11	94.4	94.2	93.1	94.2	94.5	93.4	94.6	93.5	93.7	94.0	94.3	93.5
0.23	94.4	94.2	90.5	90.1	95.2	94.5	94.6	93.5	90.6	90.1	95.1	94.8
0.34	94.4	94.2	84.0	84.2	95.7	95.3	94.6	93.5	85.2	84.5	95.7	94.8
0.46	94.4	94.2	76.8	75.8	96.0	95.5	94.6	93.5	76.2	75.7	96.2	95.2
0.57	94.4	94.2	67.2	65.8	96.0	95.4	94.6	93.5	67.0	65.7	96.2	95.0
0.69	94.4	94.2	56.6	56.6	95.5	94.9	94.6	93.5	56.4	56.3	96.0	94.5
0.8	94.4	94.2	48.4	47.4	95.0	94.6	94.6	93.5	47.2	47.9	95.5	94.2
1	94.4	94.2	33.8	32.3	95.0	94.1	94.6	93.5	33.8	31.4	95.1	94.0
2	94.4	94.2	2.8	2.8	94.5	94.0	94.6	93.5	3.5	2.5	94.8	93.7
	Width ($\times 10^{-3}$)											
0	529	528	181	181	468	468	531	529	181	181	469	467
0.11	529	528	181	180	479	479	531	529	181	181	479	477
0.23	529	528	181	180	501	500	531	529	180	180	500	498
0.34	529	528	179	178	516	515	531	529	180	179	517	514
0.46	529	528	178	177	524	523	531	529	178	177	526	524
0.57	529	528	177	176	527	526	531	529	176	176	528	526
0.69	529	528	175	174	528	528	531	529	174	174	529	527
0.8	529	528	172	172	529	528	531	529	172	172	530	527
1	529	528	168	168	529	528	531	529	168	168	530	527
2	529	528	148	148	529	528	531	529	148	149	530	528

Table S8: Simulation results of Monte Carlo averages and standard deviations of the estimators for the local parameter $\eta = (\eta_0, \eta_1, \eta_2)$, the thresholds γ and c_γ, and the proportion of combining the RT and RW samples $\mathbb{P}$(comb) for the elastic combining estimator in the two cases: zero effect modification $\psi_1 = \psi_2 = 0$ (top) and nonzero effect modification $\psi_1 = \psi_2 = 1$ (bottom) with $n = 2000$ (Section 4)

Case 1: zero effect modification

	η_0		η_1		η_2		γ		c_γ		$\mathbb{P}$(comb)	
b	Est	S.D.	Est	S.D.	Est	S.D.	Est	S.D.	Est	S.D.	Est	S.D.
0	0.00	1.54	-0.01	1.98	0.01	1.99	0.30	0.44	34.04	22.87	0.68	0.47
0.11	-0.45	1.54	-0.46	1.98	-0.44	1.98	0.35	0.46	31.51	23.74	0.63	0.48
0.23	-0.94	1.55	-0.95	2.00	-0.94	2.00	0.43	0.48	27.09	24.52	0.54	0.50
0.34	-1.39	1.57	-1.40	2.02	-1.39	2.03	0.54	0.48	21.58	24.42	0.43	0.49
0.46	-1.88	1.59	-1.89	2.05	-1.88	2.06	0.67	0.45	15.26	22.70	0.30	0.46
0.57	-2.32	1.62	-2.32	2.09	-2.31	2.10	0.75	0.41	10.62	20.09	0.21	0.41
0.69	-2.80	1.66	-2.80	2.14	-2.79	2.15	0.83	0.35	6.82	16.79	0.13	0.34
0.8	-3.23	1.70	-3.23	2.20	-3.23	2.20	0.89	0.29	4.06	13.30	0.08	0.27
1	-3.98	1.77	-3.98	2.29	-3.98	2.29	0.94	0.21	1.80	8.92	0.03	0.18
2	-7.18	2.19	-7.19	2.84	-7.17	2.82	1.00	0.03	0.01	0.17	0.00	0.00

Case 2: nonzero effect modification

	η_0		η_1		η_2		γ		c_γ		$\mathbb{P}$(comb)	
b	Est	S.D.	Est	S.D.	Est	S.D.	Est	S.D.	Est	S.D.	Est	S.D.
0	0.03	1.54	0.04	1.98	0.04	1.99	0.30	0.44	34.07	22.85	0.68	0.46
0.11	-0.42	1.54	-0.41	1.99	-0.41	2.00	0.33	0.46	32.56	23.41	0.65	0.48
0.23	-0.91	1.55	-0.90	2.00	-0.90	2.01	0.41	0.48	27.94	24.43	0.56	0.50
0.34	-1.36	1.57	-1.35	2.03	-1.35	2.04	0.52	0.48	22.58	24.52	0.45	0.50
0.46	-1.84	1.59	-1.83	2.06	-1.83	2.07	0.64	0.46	16.24	23.07	0.32	0.47
0.57	-2.27	1.62	-2.27	2.10	-2.27	2.11	0.74	0.41	11.13	20.45	0.22	0.41
0.69	-2.76	1.66	-2.75	2.14	-2.75	2.16	0.83	0.35	6.98	16.98	0.13	0.34
0.8	-3.18	1.70	-3.17	2.20	-3.18	2.21	0.88	0.30	4.31	13.64	0.08	0.27
1	-3.94	1.78	-3.93	2.29	-3.94	2.30	0.94	0.22	2.00	9.41	0.04	0.19
2	-7.12	2.20	-7.11	2.84	-7.11	2.84	1.00	0.04	0.02	0.24	0.00	0.00

Table S9: Simulation results for Monte Carlo biases, standard deviations, root-mean-square errors, coverage rates and widths of 95% confidence intervals for $\widehat{\psi}_{\text{rt}}$, $\widehat{\psi}_{\text{eff}}$, and $\widehat{\psi}_{\text{elas}}$ (labeled as "RT", "Eff", and "Elastic") when the transportability of the HTE does not hold in the RW data with $n = 2000$ (Section S4.3)

	RT		Eff		Elastic	
	ψ_1	ψ_2	ψ_1	ψ_2	ψ_1	ψ_2
Bias ($\times 10^{-2}$)	0.6	1.3	7.5	-95.6	0.6	1.3
S.D. ($\times 10^{-3}$)	79	188	39	62	79	185
root-MSE ($\times 10^{-3}$)	79.5	188	84	958	79	185
Coverage rate (%)	95.0	94.2	48.6	0.0	94.6	94.4
Width ($\times 10^{-3}$)	311	730	150	233	311	728

Table S10: Sensitivity analysis of coverage rates and widths of the elastic confidence intervals to the choice of the cut-off value κ_n in the two cases: zero effect modification $\psi_1 = \psi_2 = 0$ (left) and nonzero effect modification $\psi_1 = \psi_2 = 1$ (right) with $n = 2000$ (Section 4); the narrower ECIs are bolded

	Case 1: zero effect modification				Case 2: nonzero effect modification			
	$0.5(\log n)^{1/2}$		$(\log n)^{1/2}$		$0.5(\log n)^{1/2}$		$(\log n)^{1/2}$	
b	$\psi_1 = 0$	$\psi_2 = 0$	$\psi_1 = 0$	$\psi_2 = 0$	$\psi_1 = 1$	$\psi_2 = 1$	$\psi_1 = 1$	$\psi_2 = 1$
	Coverage Rate (%)							
0	94.2	93.5	92.7	92.5	94.3	94.2	92.7	92.5
0.11	93.8	94.2	93.2	92.8	94.8	94.5	92.9	92.7
0.23	94.5	94.6	92.8	92.8	95.2	94.8	93.3	92.7
0.34	94.5	94.8	94.0	93.8	95.5	95.0	94.4	93.5
0.46	95.0	95.5	94.5	94.5	95.8	95.3	94.5	94.4
0.57	95.7	96.0	95.5	95.2	96.2	95.5	95.5	94.8
0.69	95.9	96.2	95.5	95.8	95.9	95.3	95.3	94.6
0.8	95.8	96.0	95.5	95.6	95.7	95.2	95.3	95.0
1	95.5	95.0	95.5	95.0	95.5	95.0	95.5	94.9
2	94.3	94.5	94.3	94.4	94.7	94.2	94.7	94.2
	Width ($\times 10^{-3}$)							
0	480	481	**472**	**473**	479	480	**472**	**474**
0.11	488	489	**488**	**487**	486	488	**479**	**480**
0.23	498	499	**496**	**497**	**497**	**499**	498	500
0.34	**509**	**510**	516	516	**507**	**509**	511	514
0.46	**518**	**519**	530	530	**518**	**519**	524	526
0.57	**524**	**524**	535	535	**524**	**526**	530	532
0.69	**528**	**528**	534	534	**526**	**528**	529	531
0.8	**528**	**528**	532	532	**527**	**529**	530	532
1	**528**	**528**	529	529	**528**	**530**	530	532
2	527	528	527	**527**	528	530	528	530

Table S11: Sensitivity analysis of $\mathbb{P}(T > \kappa_n)$ to the choice of the cut-off value κ_n in the two cases: zero effect modification $\psi_1 = \psi_2 = 0$ (left) and nonzero effect modification $\psi_1 = \psi_2 = 1$ (right) with $n = 2000$ (Section 4)

	Case 1: zero effect modification				Case 2: nonzero effect modification			
κ_n	$0.5(\log n)^{1/2}$		$(\log n)^{1/2}$		$0.5(\log n)^{1/2}$		$(\log n)^{1/2}$	
b	Est	S.D.	Est	S.D.	Est	S.D.	Est	S.D.
0	0.76	0.43	0.54	0.50	0.76	0.43	0.55	0.50
0.11	0.80	0.40	0.61	0.49	0.79	0.41	0.59	0.49
0.23	0.86	0.35	0.67	0.47	0.85	0.36	0.67	0.47
0.34	0.91	0.29	0.77	0.42	0.90	0.30	0.77	0.42
0.46	0.96	0.21	0.87	0.34	0.95	0.22	0.86	0.34
0.57	0.98	0.13	0.92	0.26	0.98	0.16	0.92	0.27
0.69	0.99	0.09	0.97	0.18	0.99	0.10	0.96	0.20
0.8	1.00	0.04	0.98	0.12	1.00	0.07	0.98	0.15
1	1.00	0.00	1.00	0.06	1.00	0.00	1.00	0.07
2	1.00	0.00	1.00	0.00	1.00	0.00	1.00	0.00

Table S12: Simulation results for coverage rates and widths of 95% confidence intervals in the case: nonzero effect modification $\psi_1 = \psi_2 = 1$ with $n = 2000$ when using sample splitting (Section S4.6)

	RT		Eff		Pre-testing		RT		Eff		Pre-testing	
b	$\psi_1 = 1$	$\psi_2 = 1$	$\psi_1 = 1$	$\psi_2 = 1$	$\psi_1 = 1$	$\psi_2 = 1$	$\psi_1 = 1$	$\psi_2 = 1$	$\psi_1 = 1$	$\psi_2 = 1$	$\psi_1 = 1$	$\psi_2 = 1$
	Coverage Rate (%)						Width ($\times 10^{-2}$)					
0	94.4	94.8	94.4	94.4	94.0	95.2	542	546	245	246	357	356
0.11	94.4	94.8	93.4	94.0	93.0	95.2	542	546	245	246	361	365
0.23	94.4	94.8	89.8	88.4	91.6	92.2	542	545	244	244	397	399
0.34	94.4	94.8	84.2	83.6	90.6	88.8	542	545	243	243	430	433
0.46	94.4	94.8	74.4	77.2	89.4	90.0	542	546	242	243	471	475
0.57	94.4	94.8	63.6	69.6	88.6	89.6	542	546	240	241	500	503
0.69	94.6	94.8	52.8	59.0	90.8	91.2	542	545	237	238	519	518
0.8	94.4	94.8	42.6	47.8	92.8	92.8	542	546	236	235	533	534
1	94.4	94.8	28.6	32.2	93.6	94.2	542	545	231	230	541	543
2	94.4	94.8	1.8	2.4	94.4	94.6	542	545	210	210	542	545